with the p38 MAPK inhibitor SB203580 dramatically downregulated the expression levels of *BMP2* and *FGF2* to control levels (Figure 4C and D). In contrast, the Erk1/2 MAPK inhibitor U0126 had no effect on *FGF2* expression levels and led to a slight increase in *BMP2* expression (Figure 4C and D).

MKK6-mediated activation of p38 MAPK increases BMP2 and FGF2 expression in hADMPCs

To further confirm the involvement of p38 MAPK in the regulation of BMP2 and FGF2, hADMPCs were transduced with a lentiviral vector expressing constitutively active MKK6 (MKK6 (glu)) [30] from an EF1α promoter. As shown in Figure 5A, lentiviral transduction of MKK6 (glu) led to expression of Flag-tagged MKK6 (glu) in hADMPCs. Moreover, the expression of MKK6 (glu) resulted in activation of p38 MAPK as expected [30] (Figure 5A), and upregulation of BMP2 and FGF2 expression (Figure 5B-E).

NF-κB is not activated in hADMPCs exposed to oxidative stress

It has been reported that NF-κB directly binds to the *BMP2* promoter to induce its expression [31], and MSK1, a downstream molecule of p38 MAPK, is involved in NF-κB transactivation [32]. Therefore, we

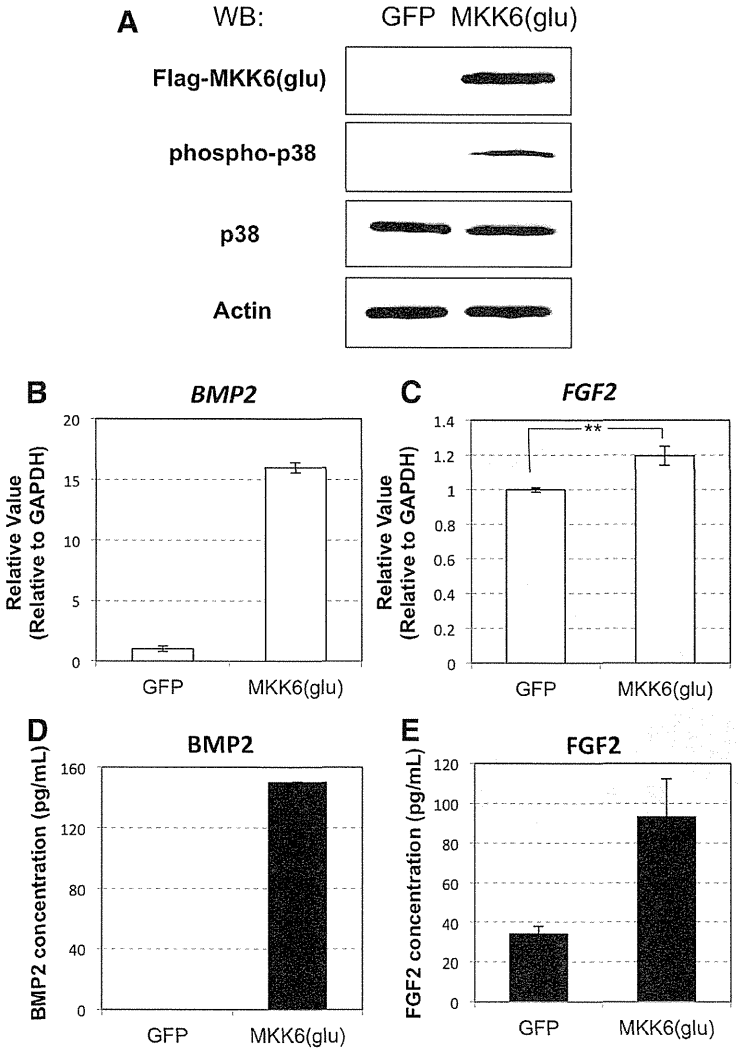

Figure 5 Activation of p38 MAPK by a constitutively active form of MKK6 resulted in elevated expression of BMP2 and FGF2. (A) A lentiviral vector expressing Flag-tagged MKK6 (glu) was transfected into hADMPCs. Expression of Flag-tagged MKK6 (glu), phosphorylated p38 MAPK and p38 MAPK was analyzed by western blotting. A CSII-EF-EGFP lentiviral vector was infected as a control (GFP). Actin was detected as an internal control. **(B, C)** Transcriptional levels of *BMP2* (**B**) and *FGF2* (**C**) were analyzed by q-PCR. The most reliable internal control gene was determined using the geNorm Software. **(D, E)** BMP2 (**D**) and FGF2 (**E**) secretion was analyzed by ELISA.

hypothesized that p38 MAPK-mediated activation of NF-κB might contribute to elevated expression of *BMP2* mRNA. To confirm this hypothesis, transcriptional activation of NF-κB was examined by measuring luciferase activity driven by the synthetic NF-κB response element. We found that transcriptional activity of NF-κB was not stimulated by BSO treatment (Figure 6A), and immunocytochemical analysis also revealed that NF-κB was not activated (nuclear localization of NF-κB/p65 was rarely observed) in BSO-treated hADMPCs (Figure 6B). These results suggested that elevated expression of *BMP2* mRNA is not mediated by NF-κB signaling.

Our current data thus demonstrate the crucial role of ROS, via activation of the p38 MAPK signaling pathway, in regulating expression levels of the neurotrophic factors BMP2 and FGF2 in hADMPCs. The overall model that we propose, based upon our findings, is shown in Figure 7.

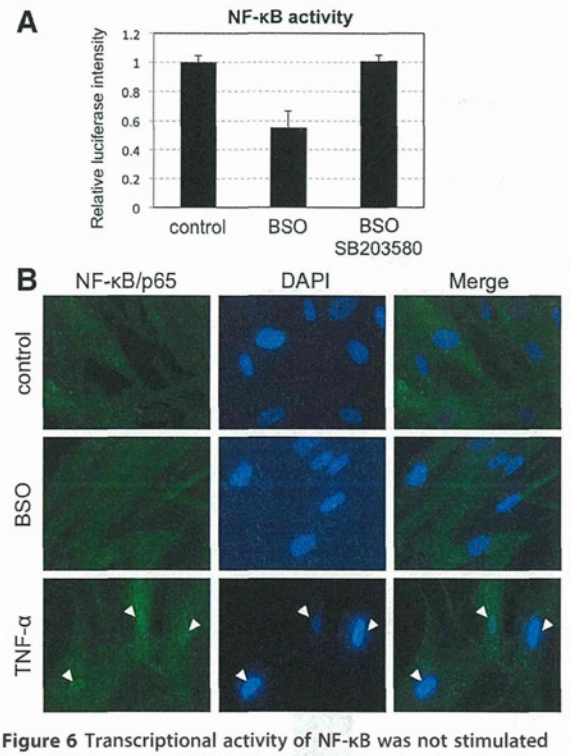

Figure 6 Transcriptional activity of NF-κB was not stimulated by oxidative stress. hADMPCs were transfected with pNF-κB-Luc and were treated with 10 μM of SB203580 or 0.1% DMSO for 2 h followed by addition of 1 mM of BSO. After 24 h, the medium was changed to fresh medium and cells were cultured for an additional 2 days. **(A)** The activity of NF-κB was measured by the intensity of luciferase activity driven from a minimal promoter containing tandem repeats of the NFκB transcriptional response element. Data shown represent the average of 3 independent experiments. **(B)** Immunocytochemical analysis against NF-κB/p65 (green). Blue staining represents nuclear staining by DAPI. Note that nuclear localization of NF-κB/p65 (white arrowhead) is only observed in hADMPCs treated with 20 ng/mL of TNF-α.

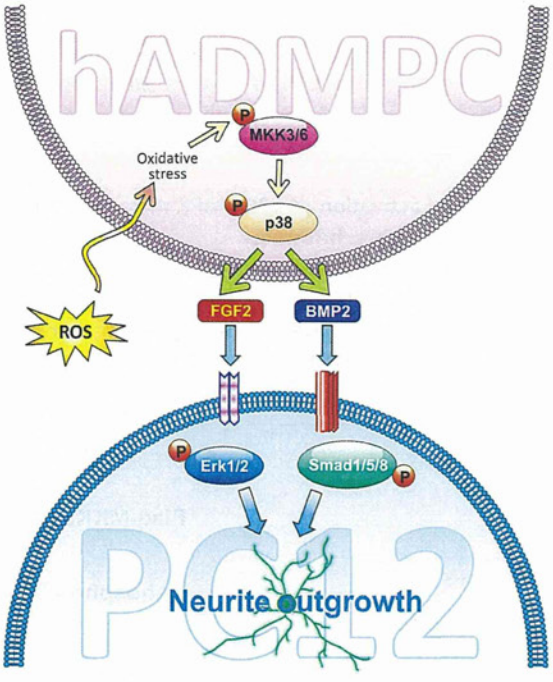

Figure 7 Model of this study. A schematic illustration of the results of this study is shown. Oxidative stress by BSO treatment in hADMPCs results in p38 MAPK activation, which then leads to BMP2 and FGF2 expression and secretion. The secreted factors then bind to the receptors on PC12 cells, facilitating neural differentiation in these cells.

Discussion

In this study, we investigated the effect of oxidative stress in hADMPCs on the induction of neuronal differentiation. Such mechanisms may explain how administration of hADMPCs to neurodegenerative lesions enhances endogenous repair mechanisms via neurogenesis of endogenous neural progenitor and stem cells. Damaged tissues, such as the brain tissue of patients who have suffered from ischemic stroke, are subject to inflammation and the generation of reactive oxygen species (ROS) [17,18]. Our data demonstrated that hADMPCs, when exposed to oxidative stress, facilitate neuronal differentiation in rat pheochromocytoma cell line PC12 cells by upregulation of fibroblast growth factor 2 (FGF2) and bone morphogenetic protein 2 (BMP2) secretion through p38 MAPK activation.

Our results show that BMP2 and FGF2 were upregulated in hADMPCs when exposed to buthionine sulfoximine (BSO), a glutathione-synthesis inhibitor that leads to oxidative stress. These findings may have therapeutic implications in neurodegenerative diseases. We concluded that BMP2 and FGF2 secreted from hADMPCs that had been exposed to oxidative stress were the main inducers of neurite outgrowth in PC12 cells. Erk1/2 and

Smad1/5/8 were significantly activated in these cells (Figure 2), while other growth factors known to induce neurite outgrowth in PC12 cells such as nerve growth factor (NGF) and vascular endothelial growth factor (VEGF) were not observed to be upregulated by BSO treatment (data not shown). We confirmed that BMP2 enhanced the effect that FGF2 had on the differentiation of PC12 cells (Figure 3), supporting our idea that hADMPCs under oxidative stress conditions secrete BMP2 and FGF2 and that this contributes to neuronal differentiation. Consistent with our conclusions, it has been reported that BMP2, via activation of a Smad signaling pathway, facilitated FGF2-induced neuronal differentiation in PC12 cells [26,27]. However, since hADMPCs have been reported to secrete many growth factor including NGF, VEGF, HGF, and IGF [11,15,33], we cannot exclude the possibility that BMP2 and FGF2 are acting cooperatively with these growth factors to facilitate neurite outgrowth in PC12 cells. Thus, the precise molecular mechanisms of induction of PC12 differentiation and the precise expression profiles in BSO-treated hADMPCs need to be further investigated.

Recently, BMP signaling through Smad1/5/8 has been reported to contribute to neurite outgrowth in dorsal root ganglion neurons both in vitro and in vivo [34,35]. Moreover, BMP2 has been shown to have neurotrophic effects on midbrain dopaminergic neurons [36], ventral mesencephalic neurons [37], mouse embryonic striatal neurons [38], and nitrergic and catecholaminergic enteric neurons [39]. Moreover, FGF2 is trophic for neurons, glias, and endothelial cells in the central nervous system. FGF2 also prevents downregulation of the antiapoptotic protein Bcl-2 in ischemic brain tissue and limits excitotoxic damage to the brain through an activin-dependent mechanism [40]. These findings are consistent with our hypothesis that hADMPCs secret BMP2 and FGF2 to induce neurogenesis in neurodegenerative lesions in response to oxidative stress.

As it has been shown that ROS activate ERKs, JNKs, and p38 MAPKs [28,29], we examined the MAPK signaling pathway in hADMPCs exposed to oxidative stress and found that BSO treatment resulted in significant activation of ERK1/2 and p38 MAPK. Intriguingly, addition of SB203580, a specific inhibitor of p38 MAPK, but not the ERK inhibitor U0126, suppressed *BMP2* and *FGF2* expression in BSO-treated hADMPCs to control levels (Figure 4), suggesting that p38 MAPK was contributing to upregulation of BMP2 and FGF2 in hADMPCs when exposed to oxidative stress. Moreover, lentiviral transduction of the constitutively active form of MKK6, a MAPKK that selectively activates p38 MAPK isoforms [30], resulted in upregulation of BMP2 and FGF2 and this also demonstrated the crucial role of the p38 MAPK cascade in the regulation of BMP2 and FGF2. In primary human endothelial cells, p38-dependent regulation of BMP2 expression was reported previously. Viemann *et al.* [41] investigated the genes that were induced by inflammatory stimulation with tumor necrosis factor α (TNF-α) and classified these genes into 2 categories based on whether they were regulated in an NF-κB-dependent or p38 MAPK-dependent manner. Consistent with our findings, they found that significant induction of BMP2 expression by TNF-α was markedly suppressed by SB202190, an inhibitor of p38 MAPK. These results support the hypothesis that activation of the p38 MAPK pathway in hADMPCs in response to inflammation surrounding neurodegenerative lesions leads to induction of BMP2 and FGF2, which in turn support regeneration of neuronal cells.

It has been known that NF-κB directly binds to the BMP2 promoter to induce its expression [31], and MSK1, a downstream molecule of p38 MAPK, is involved in NF-κB transactivation [32]. However, we did not observe an elevation of NF-κB transcriptional activity in hADMPCs when they were exposed to oxidative stress (Figure 6). The mechanism of p38-dependent regulation of gene expression is not completely understood, and the precise mechanism by which p38 MAPK regulates the expression of BMP2 and FGF2 remains to be determined.

In this study, we also found that suppression of ERK1/2 MAPK by U0126 in BSO-treated hADMPCs resulted in slight activation of p38 MAPK (Figure 4A). Consistent with this, the expression level of *BMP2* mRNA was also upregulated when cells exposed to oxidative stress were pretreated with U0126 (Figure 4C). Previously, "seesaw cross-talk" between ERK and p38 MAPK signaling has been reported; i.e., the MEK inhibitor caused a decrease in the phosphorylation level of ERK and an increase in that of p38, whereas the p38 inhibitor had the opposite effect [42-44]. We did not investigate the phosphorylation of ERK1/2 in SB203580-treated hADMPCs, but it may be possible that seesaw cross-talk also occurs in our system.

Conclusions

In summary, the results obtained in this study have demonstrated the potential use of hADMPCs for the treatment of neurodegenerative diseases such as ischemic stroke, Parkinson's disease, Alzheimer's disease, and spinal cord injury, in which the transplanted hADMPCs might be exposed to oxidative stress. Moreover, the p38-dependent modulation of BMP2 and FGF2 expression observed in this study is expected to be a new therapeutic target for neurodegenerative disorders.

Materials and methods

Adipose tissue samples

Subcutaneous adipose tissue samples (10–50 g, each) were resected during plastic surgery in 5 females (age,

20–60 years) as excess discards. The study protocol was approved by the Review Board for Human Research of Kobe University Graduate School of Medicine, Foundation for Biomedical Research and Innovation and Kinki University Pharmaceutical Research and Technology Institute (reference number: 10–005). Each subject provided a signed informed consent.

Cell culture

PC12 cells were obtained from the Health Science Research Resources Bank (Osaka, Japan) and maintained in RPMI1640 media supplemented with 10% heat-inactivated horse serum and 5% fetal bovine serum. For differentiation, the cells were plated in 6-well culture plates coated with collagen type I (Nitta Gelatin, Osaka, Japan) and the medium was replaced with differentiation medium (RPMI1640 supplemented with 1% horse serum and 0.5% fetal bovine serum) or conditioned medium from hADMPCs. NGF (50 ng/mL), BMP2 (40 ng/mL) or FGF2 (5 ng/mL) were added to the differentiation medium. Recombinant murine Noggin (200 ng/mL: PeproTech, NJ, USA) was added to conditioned medium from BSO-treated hADMPCs. hADMPCs were isolated as previously reported [4-6,45,46] and maintained in a medium containing 60% DMEM-low glucose, 40% MCDB-201 medium (Sigma Aldrich, St. Louis, MO, USA), 1× insulin-transferrin-selenium (Gibco Invitrogen, NY, USA), 1 nM dexamethasone (Sigma Aldrich), 100 mM ascorbic acid 2-phosphate (Wako, Osaka, Japan), 10 ng/mL epidermal growth factor (PeproTech), and 5% fetal bovine serum. The cells were plated to a density of 5×10^3 cells/cm^2 on fibronectin-coated dishes, and the medium was replaced every 2 days.

Preparation of conditioned medium from hADMPCs

Two days after plating, hADMPCs were treated with BSO (concentrations used were varied in each experiment and are indicated in the results and figure legends) for 16 h. The medium was replaced with fresh culture medium for 2 days followed by replacement with PC12 cell differentiation medium. After 2 more days, the medium was removed for use as conditioned medium. For preparation of the conditioned medium from hADMPCs in which one of the three, p38, Erk1/2, or JNK MAPK, was inhibited, hADMPCs were pretreated with 10 μM SB203580 (Promega, WI, USA), 10 μM U0126 (Promega), or 10 μM JNK inhibitor II (EMD4 Bioscience, CA, USA), respectively, for 2 h and subsequently treated with 1 mM BSO.

Measurement of GSH/GSSG ratio

Ratios of reduced glutathione (GSH) to oxidized glutathione (GSSG) were measured using the GSH/GSSG-Glo assay kit (Promega) following the manufacturer's protocol.

Measurement of reactive oxygen species production

Cells were harvested and incubated with 10 μM 5-(and-6)-chloromethyl-2′,7′-dichlorodihydrofluorescein diacetate, acetyl ester (CM-H_2DCFDA). The amount of intracellular ROS production was proportional to green fluorescence, as analyzed with a Guava easyCyte 8HT flow cytometer (Millipore) using an argon laser at 488 nm and a 525/30 nm band pass filter, and dead cells were excluded with the LIVE/DEAD fixable far red dead cell stain kit (Invitrogen).

Western blot analysis

Cells were washed with ice-cold phosphate-buffered saline and lysed with M-PER Mammalian Protein Extraction Reagent (Thermo Scientific Pierce, IL, USA) following the manufacturer's instructions. Equal amounts of proteins were separated by sodium dodecylsulfate polyacrylamide gel electrophoresis (SDS-PAGE), transferred to polyvinylidene fluoride (PVDF) membranes (Immobilon-P; Millipore, MA, USA), and probed with antibodies against phospho-Erk1/2 (#4370), Erk1/2 (#4695), phospho-38 (#9215), p38 (#9212), phospho-Smad1/5/8 (#9511), phospho-Akt (#4060), Akt (#4691), phospho-JNK (#9251), JNK (#9258) (all from Cell Signaling Technology, MA, USA) and actin (Millipore). Horseradish peroxidase (HRP)-conjugated anti-rabbit and anti-mouse secondary antibodies (Cell Signaling Technology, Danvers, MA, USA) were used as probes and immunoreactive bands were visualized with the Immobilon Western Chemiluminescent HRP substrate (Millipore). The band intensity was measured using ImageJ software.

RNA extraction, cDNA generation, and quantitative polymerase chain reaction (q-PCR)

Total RNA was extracted using the RNeasy Mini Kit (Qiagen, Hilden, Germany) following the manufacturer's instructions. cDNA was generated from 1 μg of total RNA using the Verso cDNA Synthesis Kit (Thermo Scientific) and purified with the MinElute PCR Purification Kit (Qiagen). Q-PCR analysis was carried out using the SsoFast EvaGreen supermix (Bio-Rad, CA, USA) according to the manufacturer's protocols. The relative expression value of each gene was calculated using a ΔΔCt method and the most reliable internal control gene was determined using the geNorm Software (http://medgen.ugent.be/~jvdesomp/genorm/). Details of the primers used in these experiments are available on request.

Enzyme-linked immunosorbent assay

Enzyme-linked immunosorbent assay (ELISA) was performed using the Quantikine BMP-2 Immunoassay System and Quantikine FGF-2 Immunoassay System (R&D

Systems, MN, USA) following the manufacturer's protocols.

Plasmid construction and lentivirus production

Flag-tagged MKK6 (glu) [30] was provided by Addgene (pcDNA3-Flag MKK6 (glu); Addgene plasmid 13518). Flag-tagged MKK6 (glu) was cloned into a pENTR11 vector (Invitrogen). An iresGFP fragment was subsequently cloned into the plasmid to produce the entry vector pENTR11-MKK6 (glu)-iresGFP. The entry vector and CSII-EF-RfA (kindly provided by Dr. Miyoshi, RIKEN BioResource Center, Tsukuba, Japan) were incubated with LR clonase II enzyme mix (Invitrogen) to generate CSII-EF-MKK6 (glu)-iresGFP. The resultant plasmid was mixed with packaging plasmids (pCAG-HIVg/p and pCMV-VSVG-RSV-Rev, kindly provided by Dr. Miyoshi) and transfected into 293 T cells. The supernatant medium, which contained lentiviral vectors, was collected 2 days after transduction and concentrated by centrifugation (6000 G, 15 h, 4°C).

Luciferase assay

hADMPCs were transfected with pGL4.74 (Promega) and either pTAL-Luc or pNF-κB-Luc by TransIT-2020 (TaKaRa-Bio). The cells were then treated with 10 μM of SB203580 or 0.1% DMSO for 2 h followed by addition of 1 mM of BSO. After 24 h, the medium was changed to fresh medium and cells were cultured for an additional 2 days. The activity of NF-κB was measured using the Dual Luciferases Assay System (Promega) according to the manufacturer's protocol.

Immunocytochemistry

hADMPCs were fixed with 4% paraformaldehyde in PBS for 10 min at 4°C and then washed 3 times in PBS. Blocking was performed with PBSMT (PBS containing 0.1% Triton X-100, 2% Skim Milk) for 1 h at room temperature. The cells were then incubated with rabbit monoclonal antibody against NF-κB p65 (Cell Signaling; #8242; 1/100 dilution) overnight at 4°C. After washing with PBS, cells were incubated with Alexa 488 conjugated anti-rabbit IgG (Invitrogen; 1/1000 dilution) for 1 h. The cells were counterstained with 4'-6-diamidino-2-phenylindole (DAPI) (Invitrogen) to identify cellular nuclei.

Competing interests

None of the authors have any competing interests related to the manuscript.

Authors' contributions

MM carried out the FACS analysis, qPCR analysis, ELISA, immunofluorescent staining, and cell culture, participated in the study design, and drafted the manuscript. HM participated in the study design, carried out the western blot analysis, luciferase assay, and cell culture, and drafted the manuscript. AU carried out western blot analysis, constructed the plasmids, and generated the lentiviral vectors. YN carried out qPCR analysis and performed the statistical analysis. AI resected subcutaneous adipose tissue samples during plastic surgery. HO and AM isolated hADMPCs from human adipose tissues. TH conceived the study, participated in its design and coordination, and helped to draft the manuscript. All authors read and approved the final manuscript.

Acknowledgements

We thank A Nishikawa, T Fukase, T Sasaki, T Shoji, K Nakagita, S Fukui, and K Honjo for technical support. We thank Dr. Roger Davis for providing the pcDNA3-Flag MKK6 (glu) plasmid and Dr. Hiroyuki Miyoshi for the CSII-EF-RfA, pCMV-VSVG-RSV-Rev and pCMV-HIVg/p plasmids. This work was supported in part by grants from the Ministry of Health, Labor, and Welfare of Japan and a grant from the Program for Promotion of Fundamental Studies in Health Sciences of the National Institute of Biomedical Innovation (NIBIO).

Author details

[1]Pharmaceutical Research and Technology Institute, Kinki University, 3-4-1 Kowakae, Higashi-Osaka, Osaka 577-8502, Japan. [2]Department of Somatic Stem Cell Therapy and Health Policy, Foundation for Biomedical Research and Innovation, TRI305, 1-5-4 Minatojima-minamimachi, Chuo-ku, Kobe, Hyogo 650-0047, Japan. [3]Department of Plastic Surgery, Kobe University Hospital, Kobe, Japan.

Received: 28 March 2012 Accepted: 2 August 2012
Published: 7 August 2012

References

1. Pittenger MF, Mackay AM, Beck SC, Jaiswal RK, Douglas R, Mosca JD, Moorman MA, Simonetti DW, Craig S, Marshak DR: **Multilineage potential of adult human mesenchymal stem cells.** *Science* 1999, **284**:143–147.
2. Bieback K, Kern S, Kluter H, Eichler H: **Critical parameters for the isolation of mesenchymal stem cells from umbilical cord blood.** *Stem Cells* 2004, **22**:625–634.
3. Zuk PA, Zhu M, Ashjian P, De Ugarte DA, Huang JI, Mizuno H, Alfonso ZC, Fraser JK, Benhaim P, Hedrick MH: **Human adipose tissue is a source of multipotent stem cells.** *Mol Biol Cell* 2002, **13**:4279–4295.
4. Okura H, Komoda H, Saga A, Kakuta-Yamamoto A, Hamada Y, Fumimoto Y, Lee CM, Ichinose A, Sawa Y, Matsuyama A: **Properties of hepatocyte-like cell clusters from human adipose tissue-derived mesenchymal stem cells.** *Tissue Eng Part C Methods* 2010, **16**:761–770.
5. Okura H, Matsuyama A, Lee CM, Saga A, Kakuta-Yamamoto A, Nagao A, Sougawa N, Sekiya N, Takekita K, Shudo Y, *et al*: **Cardiomyoblast-like cells differentiated from human adipose tissue-derived mesenchymal stem cells improve left ventricular dysfunction and survival in a rat myocardial infarction model.** *Tissue Eng Part C Methods* 2010, **16**:417–425.
6. Komoda H, Okura H, Lee CM, Sougawa N, Iwayama T, Hashikawa T, Saga A, Yamamoto-Kakuta A, Ichinose A, Murakami S, Sawa Y, Matsuyama A: **Reduction of N-glycolylneuraminic acid xenoantigen on human adipose tissue-derived stromal cells/mesenchymal stem cells leads to safer and more useful cell sources for various stem cell therapies.** *Tissue Eng Part A* 2010, **16**:1143–1155.
7. Okura H, Komoda H, Fumimoto Y, Lee CM, Nishida T, Sawa Y, Matsuyama A: **Transdifferentiation of human adipose tissue-derived stromal cells into insulin-producing clusters.** *J Artif Organs* 2009, **12**:123–130.
8. Safford KM, Safford SD, Gimble JM, Shetty AK, Rice HE: **Characterization of neuronal/glial differentiation of murine adipose-derived adult stromal cells.** *Exp Neurol* 2004, **187**:319–328.
9. Leu S, Lin YC, Yuen CM, Yen CH, Kao YH, Sun CK, Yip HK: **Adipose-derived mesenchymal stem cells markedly attenuate brain infarct size and improve neurological function in rats.** *J Transl Med* 2010, **8**:63.
10. Ikegame Y, Yamashita K, Hayashi S, Mizuno H, Tawada M, You F, Yamada K, Tanaka Y, Egashira Y, Nakashima S, Yoshimura S, Iwama T: **Comparison of mesenchymal stem cells from adipose tissue and bone marrow for ischemic stroke therapy.** *Cytotherapy* 2011, **13**:675–685.
11. Tan B, Luan Z, Wei X, He Y, Wei G, Johnstone BH, Farlow M, Du Y: **AMP-activated kinase mediates adipose stem cell-stimulated neuritogenesis of PC12 cells.** *Neuroscience* 2011, **181**:40–47.
12. Reid AJ, Sun M, Wiberg M, Downes S: *Terenghi G.* Kingham PJ: Nerve repair with adipose-derived stem cells protects dorsal root ganglia neurons from apoptosis. Neuroscience; 2011.

13. Rehman J, Traktuev D, Li J, Merfeld-Clauss S, Temm-Grove CJ, Bovenkerk JE, Pell CL, Johnstone BH, Considine RV, March KL: **Secretion of angiogenic and antiapoptotic factors by human adipose stromal cells.** *Circulation* 2004, **109**:1292–1298.
14. Lee EY, Xia Y, Kim WS, Kim MH, Kim TH, Kim KJ, Park BS, Sung JH: **Hypoxia-enhanced wound-healing function of adipose-derived stem cells: increase in stem cell proliferation and up-regulation of VEGF and bFGF.** *Wound Repair Regen* 2009, **17**:540–547.
15. Lu S, Lu C, Han Q, Li J, Du Z, Liao L, Zhao RC: **Adipose-derived mesenchymal stem cells protect PC12 cells from glutamate excitotoxicity-induced apoptosis by upregulation of XIAP through PI3-K/Akt activation.** *Toxicology* 2011, **279**:189–195.
16. McCoy MK, Martinez TN, Ruhn KA, Wrage PC, Keefer EW, Botterman BR, Tansey KE, Tansey MG: **Autologous transplants of Adipose-Derived Adult Stromal (ADAS) cells afford dopaminergic neuroprotection in a model of Parkinson's disease.** *Exp Neurol* 2008, **210**:14–29.
17. Flamm ES, Demopoulos HB, Seligman ML, Poser RG, Ransohoff J: **Free radicals in cerebral ischemia.** *Stroke* 1978, **9**:445–447.
18. Alexandrova ML, Bochev PG: **Oxidative stress during the chronic phase after stroke.** *Free Radic Biol Med* 2005, **39**:297–316.
19. Lambeth JD: **NOX enzymes and the biology of reactive oxygen.** *Nat Rev Immunol* 2004, **4**:181–189.
20. Simpson JE, Ince PG, Haynes LJ, Theaker R, Gelsthorpe C, Baxter L, Forster G, Lace GL, Shaw PJ, Matthews FE, Savva GM, Brayne C, Wharton SB, MRC Cognitive Function and Ageing Neuropathology Study Group: **Population variation in oxidative stress and astrocyte DNA damage in relation to Alzheimer-type pathology in the ageing brain.** *Neuropathol Appl Neurobiol* 2010, **36**:25–40.
21. Cai Z, Zhao B, Ratka A: **Oxidative Stress and beta-Amyloid Protein in Alzheimer's Disease.** *Neuromolecular Med* 2011, **13**:223–250.
22. Beal MF: **Mitochondria, oxidative damage, and inflammation in Parkinson's disease.** *Ann N Y Acad Sci* 2003, **991**:120–131.
23. Henchcliffe C, Beal MF: **Mitochondrial biology and oxidative stress in Parkinson disease pathogenesis.** *Nat Clin Pract Neurol* 2008, **4**:600–609.
24. Minghetti L, Ajmone-Cat MA, De Berardinis MA, De Simone R: **Microglial activation in chronic neurodegenerative diseases: roles of apoptotic neurons and chronic stimulation.** *Brain Res Brain Res Rev* 2005, **48**:251–256.
25. Colton CA, Chernyshev ON, Gilbert DL, Vitek MP: **Microglial contribution to oxidative stress in Alzheimer's disease.** *Ann N Y Acad Sci* 2000, **899**:292–307.
26. Hayashi H, Ishisaki A, Suzuki M, Imamura T: **BMP-2 augments FGF-induced differentiation of PC12 cells through upregulation of FGF receptor-1 expression.** *J Cell Sci* 2001, **114**:1387–1395.
27. Hayashi H, Ishisaki A, Imamura T: **Smad mediates BMP-2-induced upregulation of FGF-evoked PC12 cell differentiation.** *FEBS Lett* 2003, **536**:30–34.
28. Son Y, Cheong YK, Kim NH, Chung HT, Kang DG, Pae HO: **Mitogen-Activated Protein Kinases and Reactive Oxygen Species: How Can ROS Activate MAPK Pathways?** *J Signal Transduct* 2011, **2011**:792639.
29. Ito K, Hirao A, Arai F, Takubo K, Matsuoka S, Miyamoto K, Ohmura M, Naka K, Hosokawa K, Ikeda Y, Suda T: **Reactive oxygen species act through p38 MAPK to limit the lifespan of hematopoietic stem cells.** *Nat Med* 2006, **12**:446–451.
30. Raingeaud J, Whitmarsh AJ, Barrett T, Derijard B, Davis RJ: **MKK3- and MKK6-regulated gene expression is mediated by the p38 mitogen-activated protein kinase signal transduction pathway.** *Mol Cell Biol* 1996, **16**:1247–1255.
31. Feng JQ, Xing L, Zhang JH, Zhao M, Horn D, Chan J, Boyce BF, Harris SE, Mundy GR, Chen D: **NF-kappaB specifically activates BMP-2 gene expression in growth plate chondrocytes in vivo and in a chondrocyte cell line in vitro.** *J Biol Chem* 2003, **278**:29130–29135.
32. Vermeulen L, De Wilde G, Van Damme P: **Vanden Berghe W, Haegeman G: Transcriptional activation of the NF-kappaB p65 subunit by mitogen- and stress-activated protein kinase-1 (MSK1).** *EMBO J* 2003, **22**:1313–1324.
33. Rasmussen JG, Frobert O, Pilgaard L, Kastrup J, Simonsen U, Zachar V, Fink T: **Prolonged hypoxic culture and trypsinization increase the pro-angiogenic potential of human adipose tissue-derived stem cells.** *Cytotherapy* 2011, **13**:318–328.
34. Parikh P, Hao Y, Hosseinkhani M, Patil SB, Huntley GW, Tessier-Lavigne M, Zou H: **Regeneration of axons in injured spinal cord by activation of bone morphogenetic protein/Smad1 signaling pathway in adult neurons.** *Proc Natl Acad Sci U S A* 2011, **108**:E99–E107.
35. Ma CH, Brenner GJ, Omura T, Samad OA, Costigan M, Inquimbert P, Niederkofler V, Salie R, Sun CC, Lin HY, Arber S, Coppola G, Woolf CJ, Samad TA: **The BMP coreceptor RGMb promotes while the endogenous BMP antagonist noggin reduces neurite outgrowth and peripheral nerve regeneration by modulating BMP signaling.** *J Neurosci* 2011, **31**:18391–18400.
36. Jordan J, Bottner M, Schluesener HJ, Unsicker K, Krieglstein K: **Bone morphogenetic proteins: neurotrophic roles for midbrain dopaminergic neurons and implications of astroglial cells.** *Eur J Neurosci* 1997, **9**:1699–1709.
37. Reiriz J, Espejo M, Ventura F, Ambrosio S, Alberch J: **Bone morphogenetic protein-2 promotes dissociated effects on the number and differentiation of cultured ventral mesencephalic dopaminergic neurons.** *J Neurobiol* 1999, **38**:161–170.
38. Stull ND, Jung JW, Iacovitti L: **Induction of a dopaminergic phenotype in cultured striatal neurons by bone morphogenetic proteins.** *Brain Res Dev Brain Res* 2001, **130**:91–98.
39. Anitha M, Shahnavaz N, Qayed E, Joseph I, Gossrau G, Mwangi S, Sitaraman SV, Greene JG, Srinivasan S: **BMP2 promotes differentiation of nitrergic and catecholaminergic enteric neurons through a Smad1-dependent pathway.** *Am J Physiol Gastrointest Liver Physiol* 2010, **298**:G375–G383.
40. Ikeda N, Nonoguchi N, Zhao MZ, Watanabe T, Kajimoto Y, Furutama D, Kimura F, Dezawa M, Coffin RS, Otsuki Y, Kuroiwa T, Miyatake S: **Bone marrow stromal cells that enhanced fibroblast growth factor-2 secretion by herpes simplex virus vector improve neurological outcome after transient focal cerebral ischemia in rats.** *Stroke* 2005, **36**:2725–2730.
41. Viemann D, Goebeler M, Schmid S, Klimmek K, Sorg C, Ludwig S, Roth J: **Transcriptional profiling of IKK2/NF-kappa B- and p38 MAP kinase-dependent gene expression in TNF-alpha-stimulated primary human endothelial cells.** *Blood* 2004, **103**:3365–3373.
42. Hotokezaka H, Sakai E, Kanaoka K, Saito K, Matsuo K, Kitaura H, Yoshida N, Nakayama K: **U0126 and PD98059, specific inhibitors of MEK, accelerate differentiation of RAW264.7 cells into osteoclast-like cells.** *J Biol Chem* 2002, **277**:47366–47372.
43. Shimo T, Matsumura S, Ibaragi S, Isowa S, Kishimoto K, Mese H, Nishiyama A, Sasaki A: **Specific inhibitor of MEK-mediated cross-talk between ERK and p38 MAPK during differentiation of human osteosarcoma cells.** *J Cell Commun Signal* 2007, **1**:103–111.
44. Al-Shanti N, Stewart CE: **PD98059 enhances C2 myoblast differentiation through p38 MAPK activation: a novel role for PD98059.** *J Endocrinol* 2008, **198**:243–252.
45. Okura H, Saga A, Fumimoto Y, Soeda M, Moriyama M, Moriyama H, Nagai K, Lee CM, Yamashita S, Ichinose A, Hayakawa T, Matsuyama A: **Transplantation of human adipose tissue-derived multilineage progenitor cells reduces serum cholesterol in hyperlipidemic Watanabe rabbits.** *Tissue Eng Part C Methods* 2011, **17**:145–154.
46. Saga A, Okura H, Soeda M, Tani J, Fumimoto Y, Komoda H, Moriyama M, Moriyama H, Yamashita S, Ichinose A, Daimon T, Hayakawa T, Matsuyama A: **HMG-CoA reductase inhibitor augments the serum total cholesterol-lowering effect of human adipose tissue-derived multilineage progenitor cells in hyperlipidemic homozygous Watanabe rabbits.** *Biochem Biophys Res Commun* 2011, **412**:50–54.

doi:10.1186/1471-2121-13-21
Cite this article as: Moriyama *et al.*: Human adipose tissue-derived multilineage progenitor cells exposed to oxidative stress induce neurite outgrowth in PC12 cells through p38 MAPK signaling. *BMC Cell Biology* 2012 **13**:21.

Biomaterials 33 (2012) 4526–4534

Contents lists available at SciVerse ScienceDirect

Biomaterials

journal homepage: www.elsevier.com/locate/biomaterials

The promotion of hepatic maturation of human pluripotent stem cells in 3D co-culture using type I collagen and Swiss 3T3 cell sheets

Yasuhito Nagamoto [a,b], Katsuhisa Tashiro [b], Kazuo Takayama [a,b], Kazuo Ohashi [d], Kenji Kawabata [b,c], Fuminori Sakurai [a], Masashi Tachibana [a], Takao Hayakawa [e,f], Miho Kusuda Furue [g,h], Hiroyuki Mizuguchi [a,b,i,*]

[a] Laboratory of Biochemistry and Molecular Biology, Graduate School of Pharmaceutical Sciences, Osaka University, Osaka 565-0871, Japan
[b] Laboratory of Stem Cell Regulation, National Institute of Biomedical Innovation, Osaka 567-0085, Japan
[c] Laboratory of Biomedical Innovation, Graduate School of Pharmaceutical Sciences, Osaka University, Osaka 565-0871, Japan
[d] Institute of Advanced Biomedical Engineering and Science, Tokyo Women's Medical University, Tokyo 162-8666, Japan
[e] Pharmaceutics and Medical Devices Agency, Tokyo 100-0013, Japan
[f] Pharmaceutical Research and Technology Institute, Kinki University, Osaka 577-8502, Japan
[g] Laboratory of Cell Cultures, Department of Disease Bioresources, National Institute of Biomedical Innovation, Osaka 567-0085, Japan
[h] Laboratory of Cell Processing, Institute for Frontier Medical Sciences, Kyoto University, Kyoto 606-8507, Japan
[i] The Center for Advanced Medical Engineering and Informatics, Osaka University, Osaka 565-0871, Japan

ARTICLE INFO

Article history:
Received 16 February 2012
Accepted 3 March 2012
Available online 23 March 2012

Keywords:
Hepatocyte
Co-culture
Collagen
Fibroblast
Liver
ECM (extracellular matrix)

ABSTRACT

Hepatocyte-like cells differentiated from human embryonic stem cells (hESCs) or human induced pluripotent stem cells (hiPSCs) are known to be a useful cell source for drug screening. We recently developed an efficient hepatic differentiation method from hESCs and hiPSCs by sequential transduction of FOXA2 and HNF1α. It is known that the combination of three-dimensional (3D) culture and co-culture, namely 3D co-culture, can maintain the functions of primary hepatocytes. However, hepatic maturation of hESC- or hiPSC-derived hepatocyte-like cells (hEHs or hiPHs, respectively) by 3D co-culture systems has not been examined. Therefore, we utilized a cell sheet engineering technology to promote hepatic maturation. The gene expression levels of hepatocyte-related markers (such as cytochrome P450 enzymes and conjugating enzymes) and the amount of albumin secretion in the hEHs or hiPHs, which were 3D co-cultured with the Swiss 3T3 cell sheet, were significantly up-regulated in comparison with those in the hEHs or hiPHs cultured in a monolayer. Furthermore, we found that type I collagen synthesized in Swiss 3T3 cells plays an important role in hepatic maturation. The hEHs or hiPHs that were 3D co-cultured with the Swiss 3T3 cell sheet would be powerful tools for medical applications, such as drug screening.

1. Introduction

Several studies have recently shown the ability of human embryonic stem cells (hESCs) [1] and human induced pluripotent stem cells (hiPSCs) [2] to differentiate into hepatocyte-like cells [3–6]. Although primary human hepatocytes are generally employed for drug toxicity screening in the early phase of pharmaceutical development, these cells have some drawbacks, such as their limited range of sources, difference in variability and functions from batch to batch, and de-differentiation. Because hESC- or hiPSC-derived hepatocyte-like cells (hEHs or hiPHs, respectively) have potential to resolve these problems, they are expected to be applied to drug screening. The hepatic differentiation processes from hESCs and hiPSCs are divided into three-stages, differentiation into definitive endoderm (DE) cells, hepatoblasts, and mature hepatocytes. Hepatic differentiation methods based on the treatment of growth factors have been widely used to generate hepatocyte-like cells from hESCs or hiPSCs [5–9]. However, the hepatic differentiation efficiency is not high enough for medical applications such as drug screening [10]. To promote the efficiency of hepatic differentiation and hepatic maturation, we have developed hepatic differentiation methods that combine the transduction of transcription factor genes involved in liver development

* Corresponding author. Laboratory of Biochemistry and Molecular Biology, Graduate School of Pharmaceutical Sciences, Osaka University, 1-6 Yamadaoka, Suita, Osaka 565-0871, Japan. Tel.: +81 6 6879 8185; fax: +81 6 6879 8186.
E-mail address: mizuguch@phs.osaka-u.ac.jp (H. Mizuguchi).

0142-9612/$ – see front matter © 2012 Elsevier Ltd. All rights reserved.
doi:10.1016/j.biomaterials.2012.03.011

with stimulation by growth factors [11–13]. The hepatocyte-like cells generated by our protocols have levels of expression of hepatocyte-related genes similar to the levels in (cryopreserved) primary human hepatocytes cultured for 48 h after plating [12]. Moreover, we have recently established more efficient and simple methods for hepatic differentiation from hESCs and hiPSCs by sequential transduction of forkhead box A2 (FOXA2) and hepatocyte nuclear factor 1 homeobox A (HNF1α) (in submitted). In that recent study, we showed that the hEHs or hiPHs expressed the genes of hepatocyte-related markers at levels similar to those in primary human hepatocytes and could metabolize various types of drugs.

It is known that cell–cell interactions between hepatocytes and their surrounding cells are essential for liver development and maintenance of liver functions [14–17]. Although primary human hepatocytes rapidly lose their functions under a monolayer culture condition, they could retain their functions, such as albumin secretion and urea synthesis, in three-dimensional (3D) culture and co-culture [18–21]. Moreover, it has been reported that the primary hepatocytes maintain their functions for a long time by the combination of 3D culture and co-culture, namely 3D co-culture [22–24]. In particular, the functions of primary rat hepatocytes cultured in a 3D co-culture, were shown to be more efficiently preserved than the functions of primary rat hepatocytes cultured in monolayer a co-culture [24]. Recently, Kim et al. reported that primary rat hepatocytes are able to maintain their functions in 3D co-culture with an endothelial cell sheet [25]. To perform 3D co-culture with a cell sheet, they employed cell sheet engineering technology using temperature-responsive culture dishes grafted with a temperature-responsive polymer, poly(*N*-isopropylacrylamide). This cell sheet engineering technology make it possible to manipulate a monolayer cell sheet with the extracellular matrices (ECMs) synthesized from the cells [26]. Although 3D culture or co-culture methods have been individually applied to promote hepatic differentiation from ESCs or iPSCs [27–29], few studies have investigated the hepatic differentiation from hESCS or hiPSCs using a 3D co-culture method.

In this study, we examined whether 3D co-culture, which uses the cell sheet engineering technology, could promote hepatic differentiation, and particularly the differentiation into mature hepatocyte-like cells, from hESCs and hiPSCs. Because Swiss 3T3 cells are widely used for co-culture with primary hepatocytes [18–20], we employed Swiss 3T3 cells for 3D co-culture with the hEHs or hiPHs. After hEHs and hiPHs were 3D co-cultured with a Swiss 3T3 cell sheet, we examined the expression levels of hepatocyte-related genes. Moreover, we investigated a Swiss 3T3 cell-derived factor that can promote hepatic maturation from hESCs and hiPSCs.

2. Materials and methods

2.1. hESC and hiPSC culture

A hESC line, H9 (WiCell Research Institute), was maintained on a feeder layer of mitomycin C (MMC)-treated mouse embryonic fibroblasts (MEF, Millipore) with ReproStem (ReproCELL) supplemented with 5 ng/ml fibroblast growth factor 2 (FGF2) (Sigma). hESCs were dissociated with 0.1 mg/ml dispase (Roche Diagnostics) into small clumps and were then subcultured every 4 or 5 days. H9 cells were was used following the Guidelines for Derivation and Utilization of Human Embryonic Stem Cells of the Ministry of Education, Culture, Sports, Science and Technology of Japan. One hiPSC line generated from the human embryonic lung fibroblast cell line MCR5 was provided from the JCRB Cell Bank (Tic, JCRB Number: JCRB1331). Another hiPSC line, 201B7, generated from human dermal fibroblasts was kindly provided by Dr. S. Yamanaka (KyotoUniversity). These hiPSC lines were maintained on a feeder layer of MMC-treated MEF with iPSellon (for Tic, Cardio) or ReproStem (for 201B7, ReproCELL) supplemented with 10 ng/ml (for Tic) or 5 ng/ml (for 201B7) FGF2.hiPSCs were dissociated with 0.1 mg/ml dispase (Roche Diagnostics) into small clumps and were then subcultured every 5 or 6 days.

2.2. Swiss 3T3 cell culture

A mouse fibroblast line, Swiss 3T3, was maintained with RPMI-1640 medium (Sigma) supplemented with fetal bovine serum (10%) (FBS), streptomycin (120 μg/ml), and penicillin (200 μg/ml).

2.3. Ad vectors

The human eukaryotic translation elongation factor 1 alpha 1 (EF-1α) promoter-driven HNF1α- and FOXA2-expressing Ad vectors (Ad-HNF1α and Ad-FOXA2, respectively) were constructed previously (in submitted). All of Ad vectors contain a stretch of lysine residue (K7) peptides in the C-terminal region of the fiber knob for more efficient transduction of hESCs, hiPSCs, and DE cells, in which transduction efficiency was almost 100%, and purified as described previously [11,12,30]. The vector particle (VP) titer was determined by using a spectrophotometric method [31].

2.4. In vitro differentiation

Before the initiation of cellular differentiation, the medium of hESCs and hiPSCs was exchanged for a defined serum-free medium, hESF9, and hESCs and hiPSCs were cultured as previously reported [32]. The differentiation protocol for the induction of DE cells, hepatoblasts, and hepatocytes was based on our previous report with some modifications (in submitted). Briefly, in mesendoderm differentiation, hESCs and hiPSCs were dissociated into single cells by using Accutase (Millipore) and cultured for 2 days on Matrigel (BD Biosciences) in hESF-DIF medium (Cell Science & Technology Institute) supplemented with 10 μg/ml human recombinant insulin, 5 μg/ml human apotransferrin, 10 μM 2-mercaptoethanol, 10 μM ethanolamine, 10 μM sodium selenite, and 0.5 mg/ml bovine serum albumin (BSA) (all from Sigma) (differentiation hESF-DIF medium) containing 100 ng/ml Activin A (R&D Systems) and 10 ng/ml FGF2. To generate DE cells, hESC- or hiPSC-derived mesendoderm cells were transduced with 3000 VP/cell of Ad-FOXA2 for 1.5 h on day 2 and cultured until day 6 on Matrigel in differentiation hESF-DIF medium supplemented with 100 ng/ml Activin A and 10 ng/ml FGF2. For induction of the hepatoblasts, the hESC- or hiPSC-derived DE cells were transduced with each 1500 VP/cell of Ad-FOXA2 and Ad-HNF1α for 1.5 h on day 6 and cultured for 3 days on Matrigel in hepatocyte culture medium (HCM) (Lonza) supplemented with 30 ng/ml bone morphogenetic protein 4 (BMP4) and 20 ng/ml FGF4 (all from R&D Systems). To expand the hepatoblasts, the hepatoblasts were transduced with each 1500 VP/cell of Ad-FOXA2 and Ad-HNF1α for 1.5 h on day 9 and cultured for 3 days on Matrigel in HCM supplemented with 10 ng/ml hepatocyte growth factor (HGF), 10 ng/ml FGF1, 10 ng/ml FGF4, and 10 ng/ml FGF10 (all from R&D Systems).To induce hepatic maturation, the cells were cultured for 2 days on Matrigel in L15 medium (Invitrogen) supplemented with 8.3% tryptose phosphate broth (BD Biosciences), 10% FBS (Vita), 10 μM hydrocortisone 21-hemisuccinate (Sigma), 1 μM insulin, and 25 mM NaHCO3 (Wako) (differentiation L15 medium) containing 20 ng/ml hepatocyte growth factor (HGF), 20 ng/ml Oncostatin M (OsM) (R&D Systems), and 10^{-6} M Dexamethasone (DEX) (Sigma). As described below, the Swiss 3T3 cell sheet was stratified onto hepatocyte-like cells on day 14 and cultured in differentiation L15 medium supplemented with 20 ng/ml HGF, 20 ng/ml OsM, and 10^{-6} M DEX until day 15. On day 15, Matrigel was stratified onto the cells and cultured in differentiation L15 medium supplemented with 20 ng/ml HGF, 20 ng/ml OsM, and 10^{-6} M DEX until day 25.

2.5. Cell sheet harvesting and stratifying procedure utilizing a gelatin-coated manipulator

The stratifying protocol was performed as previously described with some modifications [25,33]. Briefly, Swiss 3T3 cells were seeded on a 24-well temperature-responsive culture plate (TRCP) (Cell Seed Inc, Tokyo) on day 12. Two days after seeding (day 14), Swiss 3T3 cells were grown to confluence. On the same day (day 14), a gelatin-coated cell sheet manipulator was placed on the Swiss 3T3 cells, and the culture temperature was reduced to 20 °C for 60 min. By removing the manipulator, cultured Swiss 3T3 cells were harvested as a contiguous cell sheet that attached on the gelatin. The Swiss 3T3 cell sheet was then stratified on the hEHs or hiPHs. The culture plate with the manipulator was incubated at room temperature for 60 min to induce adherence between the hEHs or hiPHs and Swiss 3T3 cell sheet. To dissolve the gelatin, the culture plate was incubated at 37 °C for 60 min, and this was followed by several washing steps.

2.6. RNA isolation and reverse transcription-PCR

Total RNA was isolated from the hESC- or hiPSC-derived cells using ISOGENE (Nippon Gene) according to the manufacturer's instructions. cDNA was synthesized using 500 ng of total RNA with a Superscript VILO cDNA synthesis kit (Invitrogen). Real-time RT-PCR was performed with Taqman gene expression assays or Fast SYBR Green Master Mix using an ABI Step One Plus (all from Applied Biosystems). Relative quantification was performed against a standard curve and the values were normalized against the input determined for the housekeeping gene, *glyceraldehyde 3-phosphate dehydrogenase (GAPDH)*. The primer sequences used in this study are described in Supplementary Tables 1 and 2.

2.7. Preparation of verticalsection

On day 15, the hEHs cultured with or without the Swiss 3T3 cell sheet were frozen in Tissue-Tek O.C.T. Compound (Sakura Finetek), then vertically sectioned and fixed with 4% paraformaldehyde. These sections were monitored by a phase contrast microscope (Olympus).

2.8. ELISA

hESCs or hiPSCs were differentiated into the hepatocyte-like cells as described in Fig. 1A. The culture supernatants, which were incubated for 24 h after fresh medium was added, were collected and analyzed to determine the amount of ALB secretion by ELISA. ELISA kits for ALB were purchased from Bethyl Laboratories. ELISA was performed according to the manufacturer's instructions. The amount of ALB secretion was calculated according to each standard.

2.9. Co-culture and culture in a cell culture insert system (insert-culture)

hESCs were differentiated into the hepatocyte-like cells as described in Fig. 1A until day 14, and then the hESC-derived cells were harvested and seeded onto a 6-well culture plate (Falcon) with Swiss 3T3 (1:1) in a co-culture system. In a insert-culture system, hESC-derived hepatocyte-like cells were harvested and seeded onto a 6-well culture plate alone, and Swiss 3T3 cells were plated in cell culture inserts (membrane pore size 1.0 μm; Falcon), and placed in a well of the culture palate containing hESC-derived hepatocyte-like cells. These cells were cultured in differentiation L15 medium supplemented with 20 ng/ml HGF, 20 ng/ml OsM, and 10^{-6} M DEX until day 25.

2.10. Stratification of type I collagen gel

A type I collagen gel solution was prepared as suggested by Nitta Gelatin: 7 parts of solubilized collagen in HC1 (pH 3.0) 2 parts of 5× concentrated RPMI-1640 medium, and 2 parts of reconstitution buffer (0.2 M HEPES, 0.08 M NaOH) to neutralize the collagen gel, were mixed gently but rapidly at 4 °C. Next, the hESC-derived cells were cultured in a type I collagen gel solution for 3h, and then the medium waschanged and the cells were cultured in differentiation L15 medium supplemented with 20 ng/ml HGF, 20 ng/ml OsM, and 10^{-6} M DEX until day 25.

2.11. Inhibition of collagen synthesis

hESCs were differentiated into the hepatocyte-like cells as described in Fig. 1A until stratification of the Swiss 3T3 cell sheet. After stratification of the Swiss 3T3 cell sheet, the cells were cultured in differentiation L15 medium supplemented with 20 ng/ml HGF, 20 ng/ml OsM, 10^{-6} M DEX, and 25 μM 2,2′-Bipyridyl (Wako), an inhibitor of collagen synthesis, until day 25.

2.12. Western blotting analysis

Swiss 3T3 cells were cultured with 25 μM 2,2′-Bipyridyl or solvent (0.1% DMSO) for 3 days, and these cells were then homogenized with lysis buffer (1% Nonidet P-40, 1 mM EDTA, 25 mM Tris-HCl, 5 mM NaF, and 150 mM NaCl) containing protease inhibitor mixture (Sigma-Aldrich). After being frozen and thawed, the homogenates were centrifuged at 15,000× *g* at 4 °C for 10 min, and the supernatants were collected. The lysates were subjected to SDS-PAGE on 7.5% polyacrylamide gel and were then transferred onto polyvinylidene fluoride membranes (Millipore). After the reaction was blocked with 1% skim milk in TBS containing 0.1% Tween 20 at room temperature for 1 h, the membranes were incubated with goat anti-col1a1 Ab (diluted 1/200; Santa Cruz Biotechnology) or mouse anti-β-actin Ab (diluted 1/5000; Sigma) at 4 °C overnight, followed by reaction with horseradish peroxidase-conjugated anti-goat IgG (Chemicon) or anti-mouse IgG (Cell Signaling Technology) at room temperature for 1 h. The band was visualized by ECL Plus Western blotting detection reagents (GE Healthcare) and the signals were read using a LAS-3000 imaging system (FUJI Film).

2.13. Statistical analysis

Statistical analysis was performed using the unpaired two-tailed Student's *t*-test.

3. Results

3.1. Efficient hepatic maturation by stratification of the Swiss 3T3 cell sheet

The hEHs, which were generated by the transduction of *HNF1α* and *FOXA2* genes, were 3D co-cultured with the Swiss 3T3 cell sheet to promote hepatic differentiation and to generate mature hepatocytes from hESCs and hiPSCs. Our differentiation strategy using the stratification of the Swiss 3T3 cell sheet is illustrated in Fig. 1A. The stratifying procedure was performed on day 14 as described in Fig. 1B. The day after stratifying the Swiss 3T3 cell sheet on the hEHs, vertical sections of the monolayer hEHs (hEHs-mono) and the hEHs stratified with the Swiss 3T3 cell sheet (hEHs-Swiss) were prepared (Fig. 1C). We found that Swiss 3T3 cells were successfully harvested and overlaid onto the hEHs as a monolayer cell sheet (Fig. 1C). Moreover, the hEHs seemed to be larger than the Swiss 3T3 cells. The space between the hEHs cells and Swiss 3T3 cells suggests the formation of ECMs (Fig. 1C).

To investigate whether stratification of the Swiss 3T3 cell sheet could promote hepatic maturation of the hEHs, hESCs (H9) were differentiated into the hepatocyte-like cells according to the protocol described in Fig. 1A, and then the gene expression levels of hepatocyte-related markers and the amount of albumin (ALB) secretion in the hEHs-Swiss were measured on day 25 (Fig. 2). By 3D co-culturing of the hepatocyte-like cells with the Swiss 3T3 cell sheet for 10 days (days 15–25), the gene expression levels of hepatocyte-related markers, such as *ALB* (Fig. 2A), *hepatocyte nuclear factor 4 alpha* (*HNF4A*) (Fig. 2B), cytochrome P450 (CYP) enzymes (*CYP2C9*, *CYP7A1*, *CYP1A2*, and *CYP3A5*) (Fig. 2D–G), and conjugating enzymes (*glutathione S-transferase alpha 1* [*GSTA1*], *GSTA2*, and *UDP glucuronosyltransferase* [*UGT1A1*]) (Fig. 2H–J) were significantly increased as compared with those in hEHs-mono. Moreover, the amount of ALB secretion in hEHs-Swiss was also up-regulated as compared with that in hEHs-mono (Fig. 2K). Because it is known that hepatoblasts can differentiate into hepatocytes and cholangiocytes [34,35], we examined the gene expression level of *cytokeratin 7* (*CK7*), a cholangiocyte-related marker, in hEHs-Swiss and hEHs-mono. In 3D co-culture with the Swiss 3T3 cell sheet, the gene expression level of *CK7* was down-regulated in the hEHs-Swiss relative to the hEHs-mono (Fig. 2C). These results clearly showed that stratification of the Swiss 3T3 cell sheet could promote the hepatic maturation of the hEHs and, in turn, suppress the cholangiocyte differentiation.

In order to investigate whether stratification of the Swiss 3T3 cell sheet promotes maturation of hiPHs as well as hEHs, the hiPSCs (Tic and 201B7) were differentiated into the hepatocyte-like cells according to the protocol described in Fig. 1A. The results showed that the gene expression levels of *ALB*, *CYP2C9*, *CYP3A5*, *CYP1A2*, and *GSTA1* in the hiPHs stratified with the Swiss 3T3 cell sheet (hiPHs-Swiss) were up-regulated in comparison with those in the monolayer hiPHs (hiPHs-mono) (Fig. 3A–E). Moreover, the gene expression level of *CK7* was markedly decreased in hiPHs-Swiss (Fig. 3F). The gene expression level of *ALB* in the hiPHs-Swiss differentiated from Tic was higher than that in the hiPHs-Swiss differentiated from 201B7, while the gene expression levels of CYP enzymes in the hiPHs-Swiss differentiated from Tic were lower than those in the hiPHs-Swiss differentiated from 201B7 (Fig. 3A–D). These results showed that stratification of the Swiss 3T3 cell sheet promoted hepatic maturation of both hEHs and hiPHs.

3.2. Identification of maturation factors synthesized from Swiss 3T3 cells

The data described above indicate that hepatic maturation factors were produced in Swiss 3T3 cells. To elucidate the Swiss 3T3 cell-derived hepatic maturation factors, the hEHs were cultured in cell culture-insert systems (insert-cultured), in which the hEHs were co-cultured with Swiss 3T3 cells without physical contacts, or co-cultured with Swiss 3T3 cells. Quantitative PCR analysis revealed that the gene expression levels of *ALB* and *CYP2C9* in the insert-cultured hEHs were increased in comparison with the hEHs-mono, while the expression levels of these genes were lower than

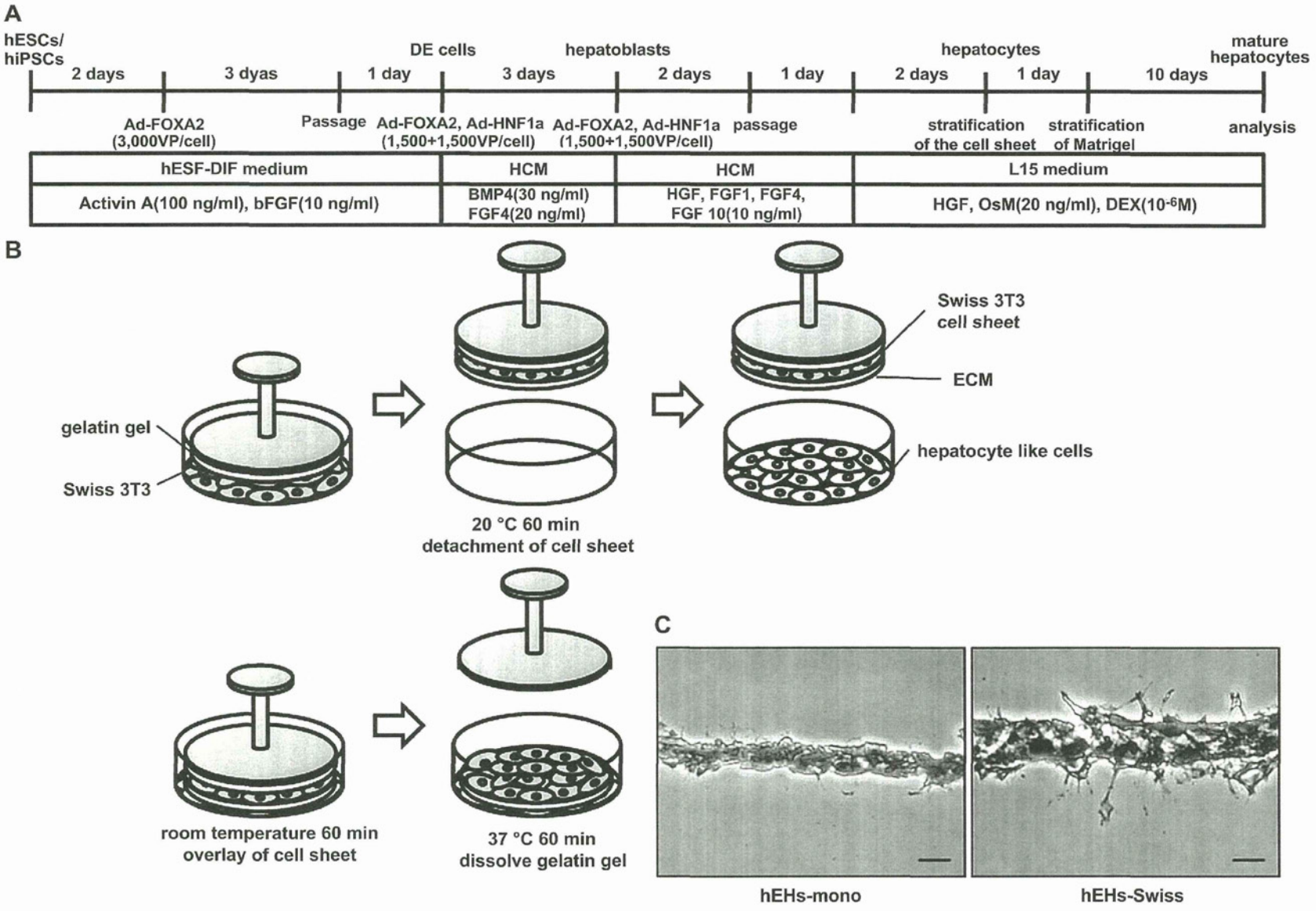

Fig. 1. Experimental protocol and schematic illustration of the procedure to stratify Swiss 3T3 cells on hepatocyte-like cells. (A) The procedure for hepatic differentiation of human embryonic stem cells (hESCs) and human induced pluripotent stem cells (hiPSCs) using stratification of the Swiss 3T3 cell sheet. Details of the hepatic differentiation procedure are described in the Materials and methods section. (B) The stratifying protocol was performed by using gelatin-coated manipulator. Details of the stratifying procedure are described in the Materials and methods section. (C) Phase-contrast micrographs of the vertical sections with monolayer hESC (H9)-derived hepatocyte-like cells (hEHs-mono) or hepatocyte-like cells stratified with Swiss 3T3 cell sheet (hEHs-Swiss) on day 15. Scale bars represent 25 μM.

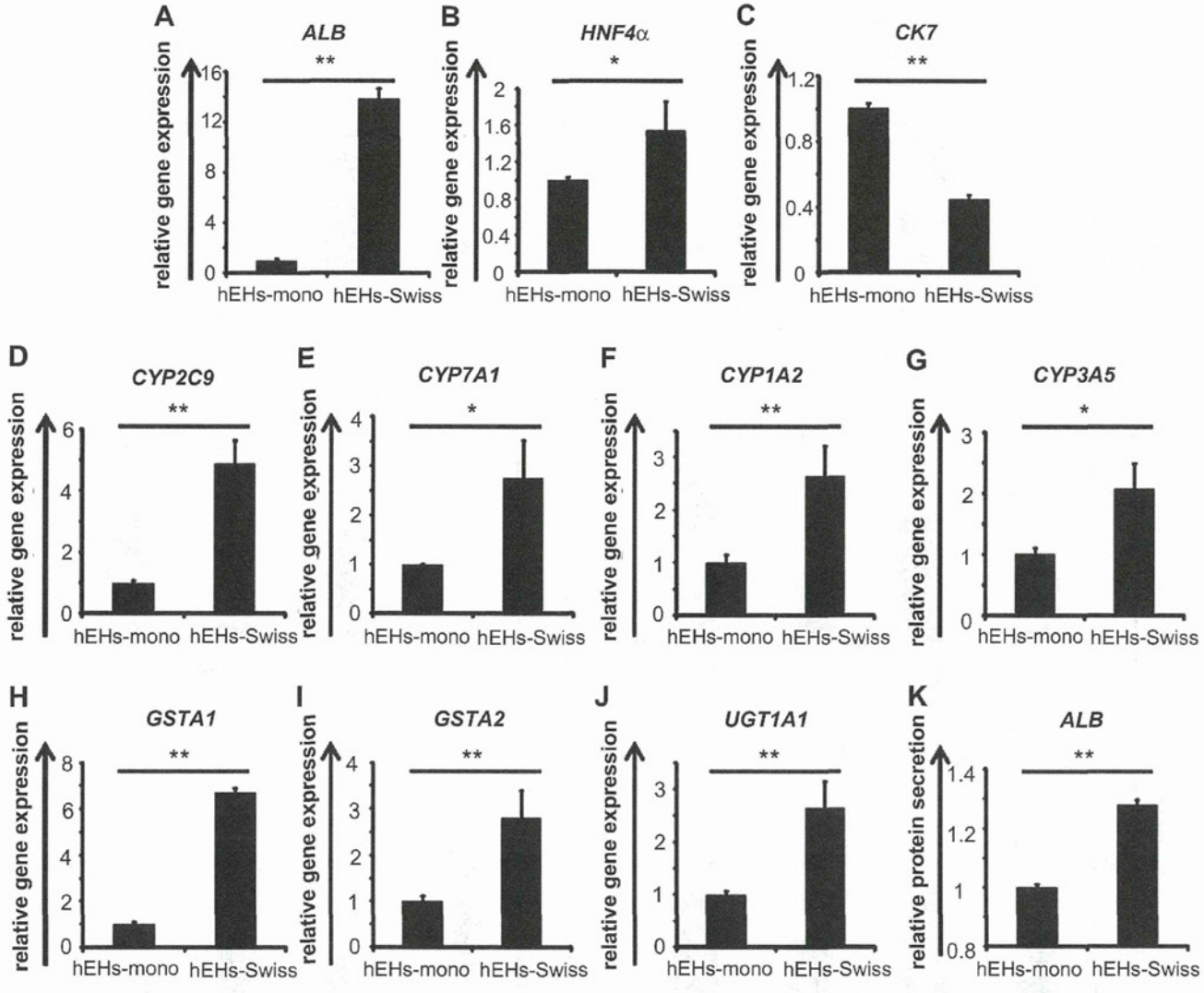

Fig. 2. Stratification of Swiss 3T3 cell sheet on hEHs promotes hepatic maturation. hESCs (H9) were differentiated into hepatocyte-like cells as described in Fig. 1A. (A–K): On day 25, the gene expression levels of *ALB* (A), *HNF4A* (B), *CK7*(C), *CYP2C9* (D), *CYP7A1* (E), *CYP1A2* (F), *CYP3A5* (G), *GSTA1* (H), *GSTA2* (I), and *UGT1A1* (J) were examined in monolayer hESC-derived hepatocyte-like cells (hEHs-mono) and hESC-derived hepatocyte-like cells stratified with Swiss 3T3 cell sheet (hEHs-Swiss) by real-time RT-PCR. The values were graphed as the fold-changes relative to hEHs-mono. (K) On day 25, the amounts of ALB secretion were examined in hEHs-mono or hEHs-Swiss by ELISA. The values were graphed as the fold-changes relative to hEHs-mono. All data are represented as means ± Standard Deviation (SD) ($n = 3$). *$P < 0.05$ **$P < 0.01$.

those in the co-cultured hEHs (Fig. 4A and B). Furthermore, a significant elevation of *CYP1A2* and *CYP3A5* gene expression was observed only in the co-cultured hEHs (Fig. 4C and D). Therefore, these data indicate that physical contacts between hEHs and Swiss 3T3 cells play an important role in hepatic maturation of the hEHs, although Swiss 3T3 cell-derived soluble factors also played a small role in the hepatic maturation.

Because ECMs are important factors in hepatic differentiation [36], we examined the effect of Swiss 3T3 cell-derived ECMs on hepatic maturation of the hEHs. Swiss 3T3 cells abundantly synthesize collagen and almost all of the synthesized collagen is type I collagen [37]. To mimic 3D co-culture with Swiss 3T3 cell sheet, type I collagen gel was stratified onto the hEHs. As a control, Matrigel, which contains abundant type IV collagen but not type I collagen, was stratified onto the hEHs. As with the case of the Swiss 3T3 cell sheet stratification, the hEHs-mono stratified with type I collagen gel showed an elevation of hepatocyte-related marker, but a reduction of cholangiocyte marker (Fig. 5A and B, hEHs-mono). In addition, stratification of type I collagen augmented the hepatic maturation of the Swiss 3T3 cell sheet-stratified hEHs (Fig. 5A and B, hEHs-Swiss). We further examined the role of Swiss 3T3 cell-derived type I collagen on hepatic maturation using 2,2′-Bipyridyl, an inhibitor of collagen synthesize. The collagen synthesis in Swiss 3T3 cells could be efficiently inhibited by treatment with 2,2′-Bipyridyl, as determined by Western blotting analysis (Fig. 5C). Quantitative RT-PCR analysis revealed that the gene expression level of *ALB* was significantly down-regulated, but that of CK7 was up-regulated in the hEHs-Swiss cultured in the presence of 2,2′-Bipyridyl (Fig. 5D and E). Taken together, our findings indicated that type I collagen, which was synthesized from Swiss 3T3 cells, was indispensable for the maturation of the hEHs by Swiss 3T3 cell sheet.

4. Discussion

Our main purpose in the current study was to develop a more efficient method for hepatic maturation of the hEHs and hiPHs, because such a method will be needed to generate more mature hepatocyte-like cells, which have potent activity to metabolize drugs, for wide-spread use of drug screening. Therefore, we

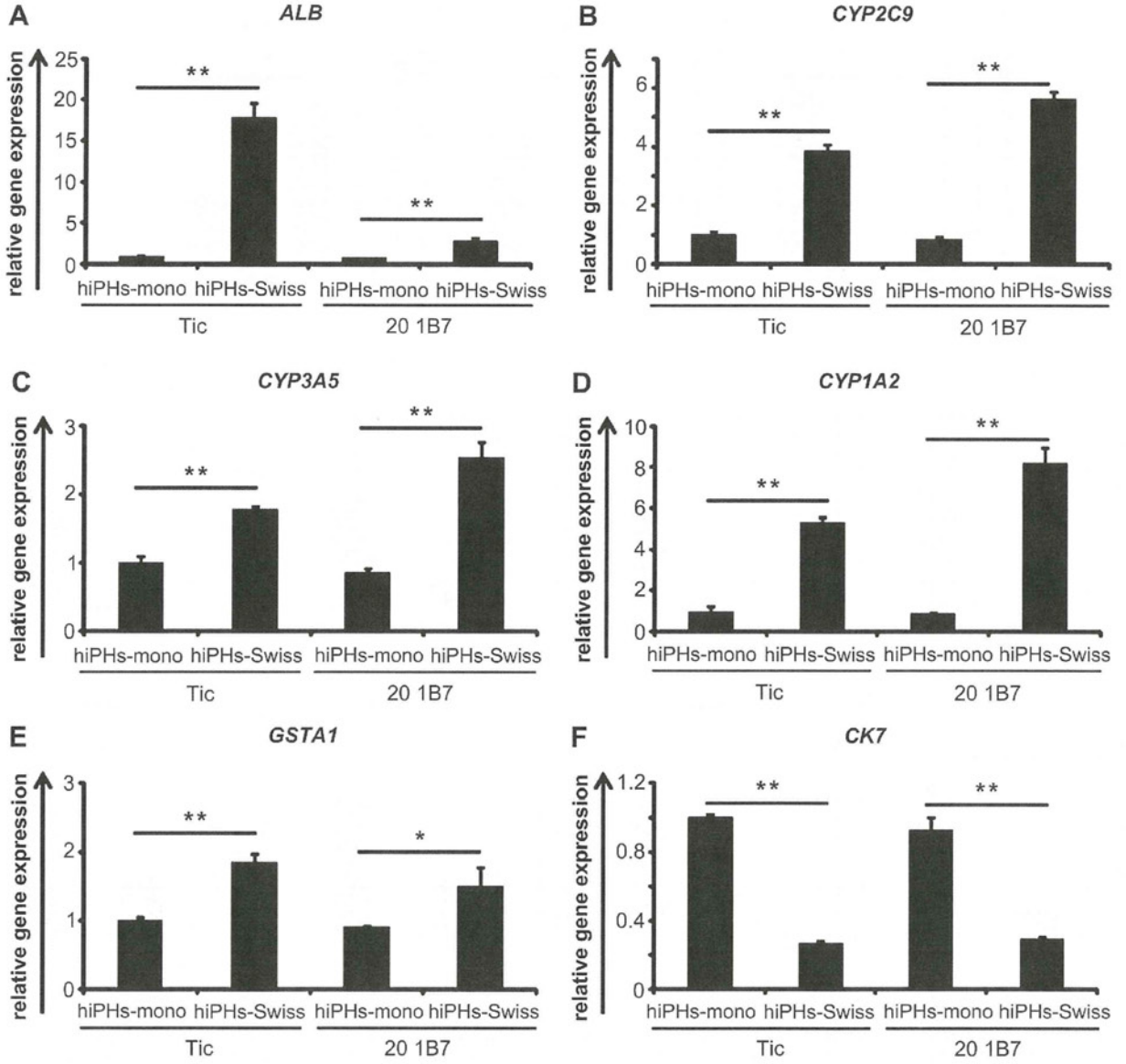

Fig. 3. Stratification of Swiss 3T3 cell sheet on hiPHs promotes hepatic maturation. Human induced pluripotent stem cells (hiPSCs) (Tic and 201B7) were differentiated into hepatocyte-like cells as described in Fig. 1A. (A–F): On day 25, the gene expression levels of *ALB* (A), *CYP2C9* (B), CYP3A5(C), *CYP1A2* (D), *GSTA1* (E), and *CK7* (F) were examined in monolayer hiPSC-derived hepatocyte-like cells (hiPHs-mono) and hiPSC-derived hepatocyte-like cells stratified with Swiss 3T3 cell sheet (hiPHs-Swiss) by real-time RT-PCR. The values were graphed as the fold-changes relative to hiPHs-mono differentiated from Tic. All data are represented as means ± SD ($n = 3$). $^{*}P < 0.05$ $^{**}P < 0.01$.

attempted to employ a cell sheet engineering technology to further induce maturation of the hEHs and hiPHs.

We observed a significant increase in the expression of hepatocyte-related genes in the hEHs- and hiPHs-Swiss as compared with those in the hEHs- and hiPHs-mono, respectively (Figs. 2 and 3), indicating that 3D co-culture with the Swiss 3T3 cell sheet was effective to promote hepatic maturation of the hEHs and hiPHs. On the other hand, Han et al. have recently shown that hESC-derived DE cells cannot be promoted to differentiate into hepatoblasts by co-culture of mouse fibroblast 3T3 cells [38]. Considering that primary rat hepatocytes are also able to grow and retain their functions for a long period of time in the presence of Swiss 3T3 cells [19,20], Swiss 3T3 cells would probably have the capacity to support the functions of freshly isolated mature hepatocytes and hESC- or hiPSC-derived hepatocyte-like cells, but not DE cells. Besides Swiss 3T3 cells, we attempted to maturate the hEHs using 3D co-culture with the bovine carotid artery endothelial cell sheet, because Kim et al. recently succeeded in creating a functional hepatocyte culture system by stacking bovine carotid artery endothelial cell sheets on primary rat hepatocytes [25]. However, our preliminary data showed that Swiss 3T3 cell sheets were superior to the bovine carotid artery endothelial cell sheets in terms of hepatic maturation of hEHs (data not shown). Thus, we conducted the present experiments to facilitate hepatic differentiation of human pluripotent stem cells using Swiss 3T3 cell sheets.

Interestingly, we found a difference in hepatic differentiation efficiency among hiPSC lines (Fig. 3). This might have been due to epigenetic memory of the hiPSC line, because several studies showed that the epigenetic memory of iPSCs affected the differentiation capacity [39,40]. Kleger et al. showed that iPSCs generated from mouse liver progenitor cells, could be more effectively differentiated into hepatocyte-like cells in comparison with iPSCs

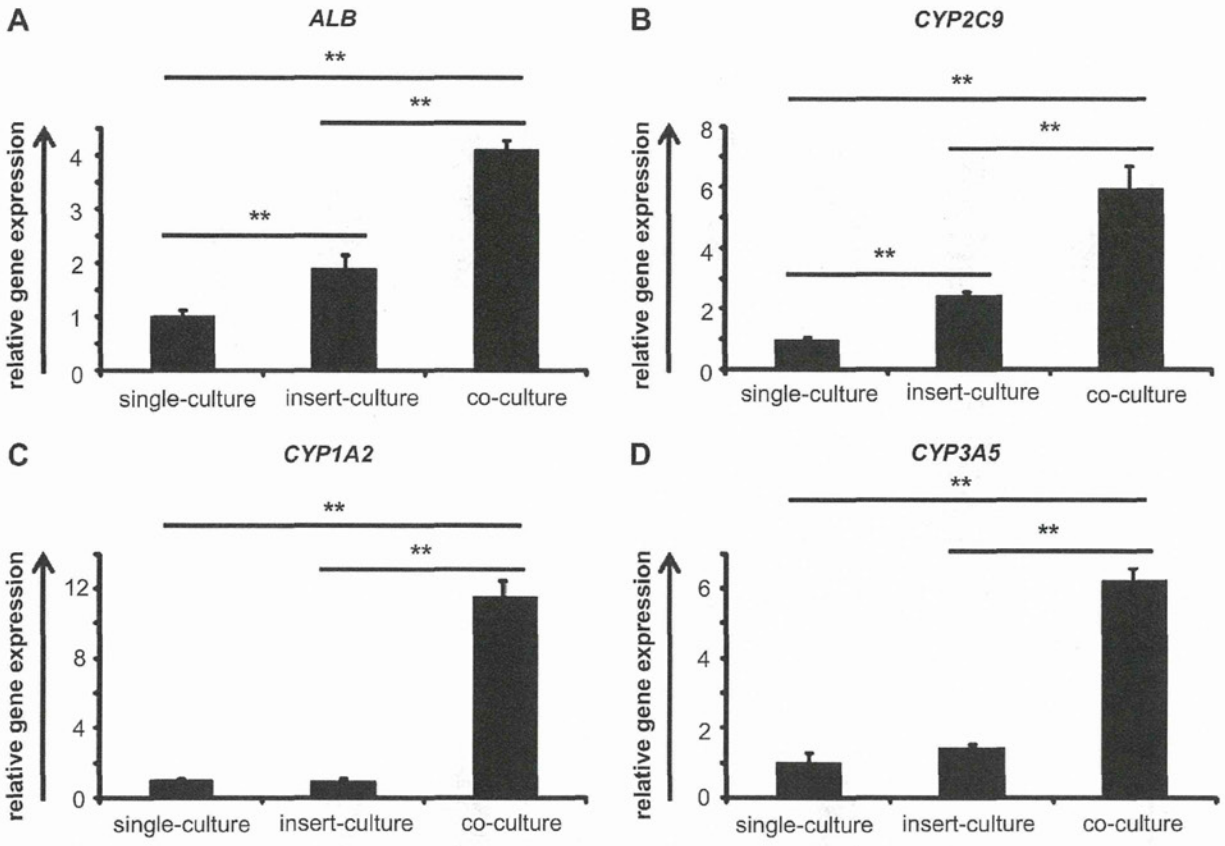

Fig. 4. Physical contacts between hESC-derived hepatocyte-like cells and Swiss 3T3 cells promote hepatic maturation. hESCs (H9) were differentiated into hepatocyte-like cells as described in Fig. 1A until day 14, and then the cells were differentiated into hepatocyte-like cells by single-culture, insert-culture, or co-culture with Swiss 3T3 cells. (A–D): On day 25, the gene expression levels of *ALB* (A), *CYP2C9* (B), *CYP1A2* (C) and *CYP3A5* (D) were examined in hESC-derived hepatocyte-like cells (hEHs) differentiated by single-culture, insert-culture, or co-culture with Swiss 3T3 cells by real-time RT-PCR. The values were graphed as the fold-changes relative to hEHs by single-culture. All data are represented as means ± SD ($n = 3$). $^{**}P < 0.01$.

generated from mouse embryo fibroblasts [41]. Thus, to more efficiently differentiate into hepatocyte-like cells from hiPSCs, it might be valuable to employ hiPSCs generated from freshly isolated human hepatocytes. Moreover, by using our 3D co-culture system, such hiPSCs would be differentiated into more mature hepatocyte-like cells.

We investigated the Swiss 3T3 cell-derived hepatic maturation factors by using cell culture inserts, and found that the physical contacts between Swiss 3T3 cells and the hEHs were the major factors contributing to the hepatic maturation of hEHs (Fig. 4). Because Swiss 3T3 cell-derived soluble factors partially induce maturation of hEHs (Fig. 4A and B), it would also be interesting to search for hepatic maturation factors secreted from Swiss 3T3 cells.

To further investigate the maturation factors, we examined whether type I collagen, which is abundantly synthesized by Swiss 3T3 cells, could promote hepatic maturation. Stratification of type I collagen gel could lead to a promotion of hepatic maturation of hEHs-mono as well as hEHs-Swiss (Fig. 5A). We also found that hepatic maturation by 3D co-culture with the Swiss 3T3 cell sheet was suppressed by inhibition of collagen synthesis (Fig. 5D). Taken together, these results show that type I collagen is one of the key molecules in promotion of hepatic maturation by stratification of Swiss 3T3 cells. It is known that the space of Disse, which faces hepatocytes directly, contains various kinds of ECM proteins, including type I collagen [42]. Because the conditions in 3D co-culture, which contains type I collagen synthesized from Swiss 3T3 cells, can mimic the *in vivo* liver microstructure, including the space of Disse, the hepatic maturation from hEHs and hiPHs might be efficiently promoted. Furthermore, it was also reported that, by the stratification of type I collagen gel in primary rat hepatocyte culture, the cytoskeletal organizations, such as actin localization, in primary rat hepatocytes were changed and stress fibers were obliterated just as in the *in vivo* state [43]. They also showed that the stratification of type I collagen gel in primary rat hepatocyte culture maintained ALB secretion in primary rat hepatocyte. Thus, the alteration of the cytoskeletal organization might also be changed in the hEHs and hiPHs by 3D co-culture with the Swiss 3T3 cell sheet. For these reasons, it could be speculated that stratification of Swiss 3T3 cell sheets positively affects the maturation process of hEHs and hiPHs mediated by cell-to-cell and cell-type I collagen–cell interactions. The expression level of the *CK7* gene in the hEHs was down-regulated by stratification of the Swiss 3T3 cell sheet or type I collagen gel (Figs. 2C and 5B). Although Matrigel, which contains large amount of type IV collagen, is widely used to differentiate hESCs and hiPSCs into hepatocyte-like cells, it is reported that type IV collagen promotes cholangiocyte differentiation [44]. Therefore, it would be important to note that stratification of Swiss 3T3 cell sheet inhibits the cholangiocyte differentiation and thereby allows the cells to drive the way to hepatic differentiation. Although we showed that a Swiss 3T3 cell-derived type I collagen plays an important role in hepatic maturation, it was likely that the other soluble factors would also be involved in the promotion of hepatic maturation.

We employed Swiss 3T3 cells for 3D co-culture with the hEHs and hiPHs. However, it would be an attractive study to employ other kinds of cells such as liver sinusoidal endothelial cells, stellate

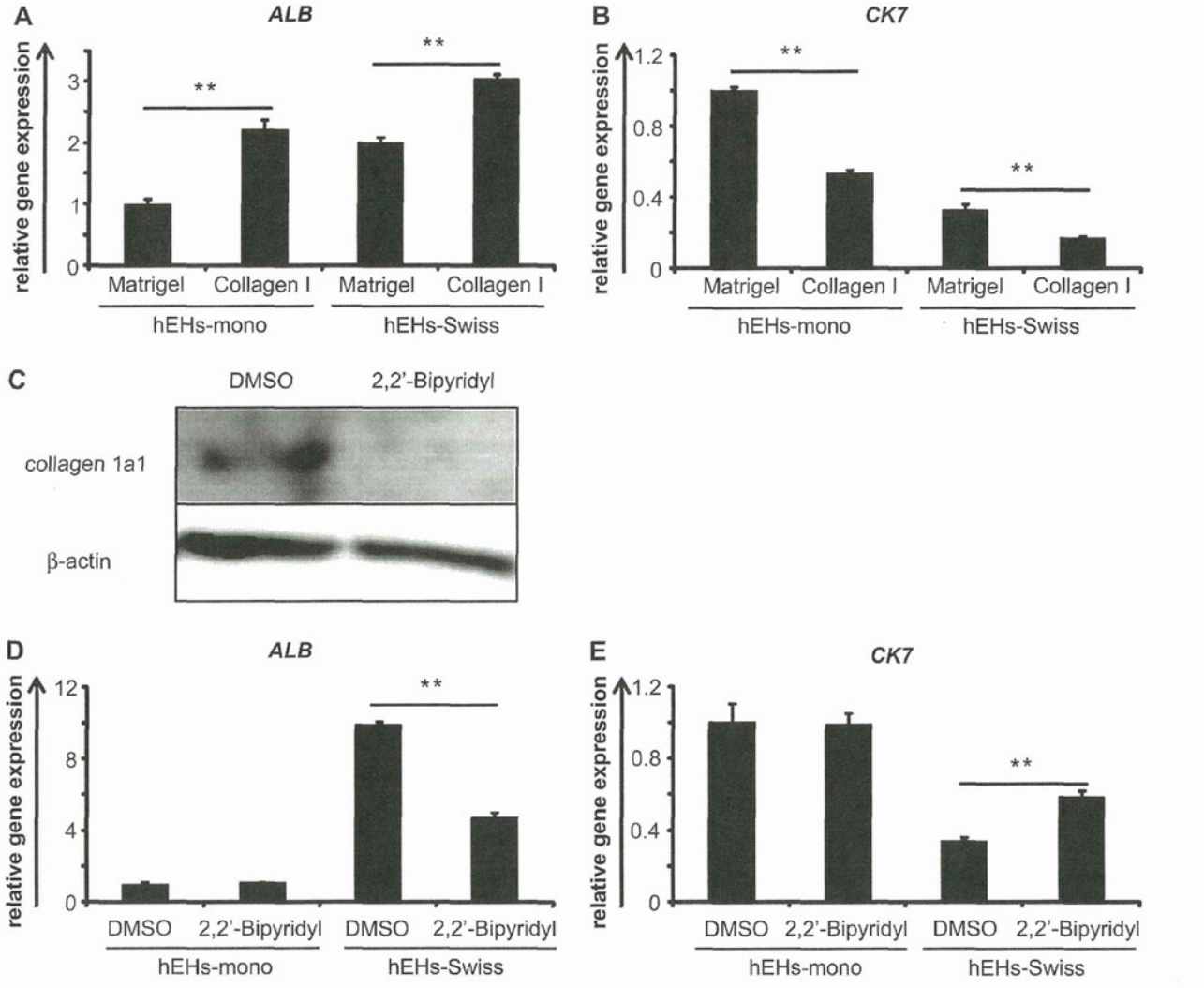

Fig. 5. Stratification of type I collagen gel promotes hepatic maturation. (A and B) hESCs (H9) were differentiated into hepatocyte-like cells as described in Fig. 1A until day 14, and then type I collagen gel (collagen I) or Matrigel are stratified on monolayer hESC-derived hepatocyte-like cells (hEHs-mono) and hESC-derived hepatocyte-like cells stratified with Swiss 3T3 cell sheet (hEHs-Swiss). On day 25, the gene expression levels of *ALB* (A) and *CK7* (B) were examined in hEHs-mono and hEHs-Swiss cultured with Matrigel or type I collagen gel by real-time RT-PCR. (C) Swiss 3T3 cells were cultured with 2,2′-Bipyridyl or solvent (0.1% DMSO) for 3 days, and then the expression of type I collagen precursor, col1a1, in these cells were detected by Western blot analysis. (D and E) hESCs (H9) were differentiated into hepatocyte-like cells as described in Fig. 1A. After stratification of Swiss 3T3 cells on day 14, these cells were treated with 2,2′-Bipyridyl or solvent (0.1% DMSO). On day 25, the gene expression levels of *ALB* (D) and *CK7* (E) were examined in hEHs-mono and hEHs-Swiss treated with 2,2′-Bipyridyl or solvent (0.1% DMSO) by real-time RT-PCR. The values were graphed as the fold-changes relative to hEHs-mono cultured with Matrigel. All data are represented as means ± SD ($n = 3$). $^{**}P < 0.01$.

cells, and Kupffer cells, to mimic the *in vivo* liver microstructure. By mimicking the *in vivo* liver microstructure, basic molecular mechanisms, including cell–cell interactions, in liver development would be clarified. Moreover, because our cell sheet technology allows us to stratify the multiple cell sheets and create layered 3D tissue constructs, combinations with multiple layers consisting of various types of cells might be able to develop an efficient method for hepatic maturation of the hEHs and hiPHs. In addition, by using new biomaterials with cell patterning techniques, more mature hepatocyte-like cells would be probably generated from human pluripotent stem cells, and thereby accelerate the research into tissue generation.

5. Conclusions

We succeeded in promoting the hepatic maturation of both the hEHs and hiPHs by stratification of the Swiss 3T3 cell sheet using a cell sheet engineering technology. We also determined that type I collagen, which is synthesized in Swiss 3T3 cells, plays an important role in hepatic maturation. Since our cell sheet engineering technology enables us to stratify multiple cell sheets, this technology would have the potential to mimic the *in vivo* liver microstructure and to generate hepatocyte-like cells, which have functions similar to primary hepatocytes. Our methods would be powerful tools for *in vitro* applications, such as drug toxicity screening in the early phase of pharmaceutical development.

Acknowledgements

We thank Misae Nishijima, Miki Yoshioka, Nobue Hirata, and Hiroko Matsumura for their excellent technical support. We also thank Tetsutaro Kikuchi (Cell Seed Inc) for providing a cell sheet stamp manipulator system. HM, KK, MKF, and TH were supported by grants from the Ministry of Health, Labor, and Welfare of Japan

(MEXT). HM was also supported by Japan Research foundation For Clinical Pharmacology and The Uehara Memorial Foundation. KO was supported by Special Coordination Funds for Promoting Science and Technology from MEXT. FS was supported by Program for Promotion of Fundamental Studies in Health Sciences of the National Institute of Biomedical Innovation (NIBIO).

Appendix A. Supplementary data

Supplementary data associated with this article can be found, in the online version, at doi:10.1016/j.biomaterials.2012.03.011.

References

[1] Thomson JA, Itskovitz-Eldor J, Shapiro SS, Waknitz MA, Swiergiel JJ, Marshall VS, et al. Embryonic stem cell lines derived from human blastocysts. Science 1998;282:1145–7.
[2] Takahashi K, Tanabe K, Ohnuki M, Narita M, Ichisaka T, Tomoda K, et al. Induction of pluripotent stem cells from adult human fibroblasts by defined factors. Cell 2007;131:861–72.
[3] Duan Y, Catana A, Meng Y, Yamamoto N, He S, Gupta S, et al. Differentiation and enrichment of hepatocyte-like cells from human embryonic stem cells in vitro and in vivo. Stem Cells 2007;25:3058–68.
[4] Touboul T, Hannan NR, Corbineau S, Martinez A, Martinet C, Branchereau S, et al. Generation of functional hepatocytes from human embryonic stem cells under chemically defined conditions that recapitulate liver development. Hepatology 2010;51:1754–65.
[5] Brolen G, Sivertsson L, Bjorquist P, Eriksson G, Ek M, Semb H, et al. Hepatocyte-like cells derived from human embryonic stem cells specifically via definitive endoderm and a progenitor stage. J Biotechnol 2010;145:284–94.
[6] Cai J, Zhao Y, Liu Y, Ye F, Song Z, Qin H, et al. Directed differentiation of human embryonic stem cells into functional hepatic cells. Hepatology 2007;45:1229–39.
[7] Snykers S, De Kock J, Rogiers V, Vanhaecke T. In vitro differentiation of embryonic and adult stem cells into hepatocytes: state of the art. Stem Cells 2009;27:577–605.
[8] Kamiya A, Kinoshita T, Miyajima A. Oncostatin M and hepatocyte growth factor induce hepatic maturation via distinct signaling pathways. FEBS Lett 2001;492:90–4.
[9] Si-Tayeb K, Lemaigre FP, Duncan SA. Organogenesis and development of the liver. Dev Cell 2010;18:175–89.
[10] Duan Y, Ma X, Zou W, Wang C, Bahbahan IS, Ahuja TP, et al. Differentiation and characterization of metabolically functioning hepatocytes from human embryonic stem cells. Stem Cells 2010;28:674–86.
[11] Inamura M, Kawabata K, Takayama K, Tashiro K, Sakurai F, Katayama K, et al. Efficient generation of hepatoblasts from human ES cells and iPS cells by transient overexpression of homeobox gene HEX. Mol Ther 2011;19:400–7.
[12] Takayama K, Inamura M, Kawabata K, Katayama K, Higuchi M, Tashiro K, et al. Efficient generation of functional hepatocytes from human embryonic stem cells and induced pluripotent stem cells by HNF4alpha transduction. Mol Ther 2012;20:127–37.
[13] Takayama K, Inamura M, Kawabata K, Tashiro K, Katayama K, Sakurai F, et al. Efficient and directive generation of two distinct endoderm lineages from human ESCs and iPSCs by differentiation stage-specific SOX17 transduction. PLoS One 2011;6:e21780.
[14] Zaret KS. Liver specification and early morphogenesis. Mech Dev 2000;92:83–8.
[15] Matsumoto K, Yoshitomi H, Rossant J, Zaret KS. Liver organogenesis promoted by endothelial cells prior to vascular function. Science 2001;294:559–63.
[16] Kinoshita T, Sekiguchi T, Xu MJ, Ito Y, Kamiya A, Tsuji K, et al. Hepatic differentiation induced by oncostatin M attenuates fetal liver hematopoiesis. Proc Natl Acad Sci USA 1999;96:7265–70.
[17] Ohashi K, Yokoyama T, Yamato M, Kuge H, Kanehiro H, Tsutsumi M, et al. Engineering functional two- and three-dimensional liver systems in vivo using hepatic tissue sheets. Nat Med 2007;13:880–5.
[18] Yamasaki C, Tateno C, Aratani A, Ohnishi C, Katayama S, Kohashi T, et al. Growth and differentiation of colony-forming human hepatocytes in vitro. J Hepatol 2006;44:749–57.
[19] Sato H, Funahashi M, Kristensen DB, Tateno C, Yoshizato K. Pleiotrophin as a Swiss 3T3 cell-derived potent mitogen for adult rat hepatocytes. Exp Cell Res 1999;246:152–64.
[20] Hui EE, Bhatia SN. Micromechanical control of cell-cell interactions. Proc Natl Acad Sci USA 2007;104:5722–6.
[21] Khetani SR, Szulgit G, Del Rio JA, Barlow C, Bhatia SN. Exploring interactions between rat hepatocytes and nonparenchymal cells using gene expression profiling. Hepatology 2004;40:545–54.
[22] Abu-Absi SF, Hansen LK, Hu WS. Three-dimensional co-culture of hepatocytes and stellate cells. Cytotechnology 2004;45:125–40.
[23] Gu J, Shi X, Zhang Y, Chu X, Hang H, Ding Y. Establishment of a three-dimensional co-culture system by porcine hepatocytes and bone marrow mesenchymal stem cells in vitro. Hepatol Res 2009;39:398–407.
[24] Thomas RJ, Bhandari R, Barrett DA, Bennett AJ, Fry JR, Powe D, et al. The effect of three-dimensional co-culture of hepatocytes and hepatic stellate cells on key hepatocyte functions in vitro. Cells Tissues Organs 2005;181:67–79.
[25] Kim K, Ohashi K, Utoh R, Kano K, Okano T. Preserved liver-specific functions of hepatocytes in 3D co-culture with endothelial cell sheets. Biomaterials 2012;33:1406–13.
[26] Harimoto M, Yamato M, Hirose M, Takahashi C, Isoi Y, Kikuchi A, et al. Novel approach for achieving double-layered cell sheets co-culture: overlaying endothelial cell sheets onto monolayer hepatocytes utilizing temperature-responsive culture dishes. J Biomed Mater Res 2002;62:464–70.
[27] Yu YD, Kim KH, Lee SG, Choi SY, Kim YC, Byun KS, et al. Hepatic differentiation from human embryonic stem cells using stromal cells. J Surg Res 2011;170:e253–61.
[28] Tuleuova N, Lee JY, Lee J, Ramanculov E, Zern MA, Revzin A. Using growth factor arrays and micropatterned co-cultures to induce hepatic differentiation of embryonic stem cells. Biomaterials 2010;31:9221–31.
[29] Miki T, Ring A, Gerlach J. Hepatic differentiation of human embryonic stem cells is promoted by three-dimensional dynamic perfusion culture conditions. Tissue Eng Part C Methods 2011;17:557–68.
[30] Kawabata K, Sakurai F, Yamaguchi T, Hayakawa T, Mizuguchi H. Efficient gene transfer into mouse embryonic stem cells with adenovirus vectors. Mol Ther 2005;12:547–54.
[31] Maizel Jr JV, White DO, Scharff MD. The polypeptides of adenovirus. I. Evidence for multiple protein components in the virion and a comparison of types 2, 7A, and 12. Virology 1968;36:115–25.
[32] Furue MK, Na J, Jackson JP, Okamoto T, Jones M, Baker D, et al. Heparin promotes the growth of human embryonic stem cells in a defined serum-free medium. Proc Natl Acad Sci USA 2008;105:13409–14.
[33] Sasagawa T, Shimizu T, Sekiya S, Haraguchi Y, Yamato M, Sawa Y, et al. Design of prevascularized three-dimensional cell-dense tissues using a cell sheet stacking manipulation technology. Biomaterials 2010;31:1646–54.
[34] Lemaigre F, Zaret KS. Liver development update: new embryo models, cell lineage control, and morphogenesis. Curr Opin Genet Dev 2004;14:582–90.
[35] Zhao R, Duncan SA. Embryonic development of the liver. Hepatology 2005;41:956–67.
[36] Suzuki A. Role for growth factors and extracellular matrix in controlling differentiation of prospectively isolated hepatic stem cells. Development 2003;130:2513–24.
[37] Goldberg B. Collagen synthesis as a marker for cell type in mouse 3T3 lines. Cell 1977;11:169–72.
[38] Han S, Dziedzic N, Gadue P, Keller GM, Gouon-Evans V. An endothelial cell niche induces hepatic specification through Dual Repression of Wnt and Notch signaling. Stem Cells 2011;29:217–28.
[39] Kim K, Doi A, Wen B, Ng K, Zhao R, Cahan P, et al. Epigenetic memory in induced pluripotent stem cells. Nature 2010;467:285–90.
[40] Polo JM, Liu S, Figueroa ME, Kulalert W, Eminli S, Tan KY, et al. Cell type of origin influences the molecular and functional properties of mouse induced pluripotent stem cells. Nat Biotechnol 2010;28:848–55.
[41] Kleger A, Mahaddalkar P, Katz SF, Lechel A, Ju JY, Loya K, et al. Increased Reprogramming capacity of mouse liver progenitor cells, compared with differentiated liver cells, Requires BAF Complex. Gastroenterology, in press.
[42] Martinez-Hernandez A. The hepatic extracellular matrix. I. Electron immunohistochemical studies in normal rat liver. Lab Invest 1984;51:57–74.
[43] Dunn JC, Tompkins RG, Yarmush ML. Long-term in vitro function of adult hepatocytes in a collagen sandwich configuration. Biotechnol Prog 1991;7:237–45.
[44] Tanimizu N, Saito H, Mostov K, Miyajima A. Long-term culture of hepatic progenitors derived from mouse Dlk+ hepatoblasts. J Cell Sci 2004;117:6425–34.

Research Article

EASL EUROPEAN ASSOCIATION FOR THE STUDY OF THE LIVER | JOURNAL OF HEPATOLOGY

Generation of metabolically functioning hepatocytes from human pluripotent stem cells by FOXA2 and HNF1α transduction

Kazuo Takayama[1,2], Mitsuru Inamura[1,2], Kenji Kawabata[2,3], Michiko Sugawara[4], Kiyomi Kikuchi[4], Maiko Higuchi[2], Yasuhito Nagamoto[1,2], Hitoshi Watanabe[1,2], Katsuhisa Tashiro[2], Fuminori Sakurai[1], Takao Hayakawa[5,6], Miho Kusuda Furue[7,8], Hiroyuki Mizuguchi[1,2,9,*]

[1]*Laboratory of Biochemistry and Molecular Biology, Graduate School of Pharmaceutical Sciences, Osaka University, Osaka 565-0871, Japan;* [2]*Laboratory of Stem Cell Regulation, National Institute of Biomedical Innovation, Osaka 567-0085, Japan;* [3]*Laboratory of Biomedical Innovation, Graduate School of Pharmaceutical Sciences, Osaka University, Osaka 565-0871, Japan;* [4]*Tsukuba Laboratories, Eisai Co., Ltd., Ibaraki 300-2635, Japan;* [5]*Pharmaceutics and Medical Devices Agency, Tokyo 100-0013, Japan;* [6]*Pharmaceutical Research and Technology Institute, Kinki University, Osaka 577-8502, Japan;* [7]*Laboratory of Cell Cultures, Department of Disease Bioresources Research, National Institute of Biomedical Innovation, Osaka 567-0085, Japan;* [8]*Laboratory of Cell Processing, Institute for Frontier Medical Sciences, Kyoto University, Kyoto 606-8507, Japan;* [9]*The Center for Advanced Medical Engineering and Informatics, Osaka University, Osaka 565-0871, Japan*

Background & Aims: Hepatocyte-like cells differentiated from human embryonic stem cells (hESCs) and induced pluripotent stem cells (hiPSCs) can be utilized as a tool for screening for hepatotoxicity in the early phase of pharmaceutical development. We have recently reported that hepatic differentiation is promoted by sequential transduction of SOX17, HEX, and HNF4α into hESC- or hiPSC-derived cells, but further maturation of hepatocyte-like cells is required for widespread use of drug screening.
Methods: To screen for hepatic differentiation-promoting factors, we tested the seven candidate genes related to liver development.
Results: The combination of two transcription factors, FOXA2 and HNF1α, promoted efficient hepatic differentiation from hESCs and hiPSCs. The expression profile of hepatocyte-related genes (such as genes encoding cytochrome P450 enzymes, conjugating enzymes, hepatic transporters, and hepatic nuclear receptors) achieved with FOXA2 and HNF1α transduction was comparable to that obtained in primary human hepatocytes. The hepatocyte-like cells generated by FOXA2 and HNF1α transduction exerted various hepatocyte functions including albumin and urea secretion, and the uptake of indocyanine green and low density lipoprotein. Moreover, these cells had the capacity to metabolize all nine tested drugs and were successfully employed to evaluate drug-induced cytotoxicity.
Conclusions: Our method employing the transduction of FOXA2 and HNF1α represents a useful tool for the efficient generation of metabolically functional hepatocytes from hESCs and hiPSCs, and the screening of drug-induced cytotoxicity.

Keywords: FOXA2; HNF1α; Hepatocytes; Adenovirus; Drug screening; Drug metabolism; hESCs; hiPSCs.
Received 14 November 2011; received in revised form 31 March 2012; accepted 4 April 2012; available online 29 May 2012
* Corresponding author. Address: Laboratory of Biochemistry and Molecular Biology, Graduate School of Pharmaceutical Sciences, Osaka University, 1-6 Yamadaoka, Suita, Osaka 565-0871, Japan. Tel.: +81 6 6879 8185; fax: +81 6 6879 8186.
E-mail address: mizuguch@phs.osaka-u.ac.jp (H. Mizuguchi).

Introduction

Hepatocyte-like cells differentiated from human embryonic stem cells (hESCs) [1] or human induced pluripotent stem cells (hiPSCs) [2] have more advantages than primary human hepatocytes (PHs) for drug screening. While application of PHs in drug screening has been hindered by lack of cellular growth, loss of function, and de-differentiation *in vitro* [3], hESC- or hiPSC-derived hepatocyte-like cells (hESC-hepa or hiPSC-hepa, respectively) have potential to solve these problems.

Hepatic differentiation from hESCs and hiPSCs can be divided into four stages: definitive endoderm (DE) differentiation, hepatic commitment, hepatic expansion, and hepatic maturation. Various growth factors are required to mimic liver development [4] and to promote hepatic differentiation. Previously, we showed that transduction of transcription factors in addition to treatment with optimal growth factors was effective to enhance hepatic differentiation [5–7]. An almost homogeneous hepatocyte population was obtained by sequential transduction of SOX17, HEX, and HNF4α into hESC- or hiPSCs-derived cells [7]. However, further maturation of the hESC-hepa and hiPSC-hepa is required for widespread use of drug screening because the drug metabolism capacity of these cells was not sufficient.

In some previous reports, hESC-hepa and hiPSC-hepa have been characterized for their hepatocyte functions in numerous ways, including functional assessment such as glycogen storage and low density lipoprotein (LDL) uptake [7]. To make a more precise judgment as to whether hESC-hepa and hiPSC-hepa can be applied to drug screening, it is more important to assess cytochrome P450 (CYP) induction potency and drug metabolism capacity rather than general hepatocyte function. Although Duan *et al.* have examined the drug metabolism capacity of hESC-hepa, drug metabolites were measured at 24 or 48 h [8]. To precisely

Molecular and Cell Biology

estimate the drug metabolism capacity, the amount of metabolites must be measured during the time when production of metabolites is linearly detected (generally before 24 h). To the best of our knowledge, there have been few reports that have examined various drugs metabolism capacity of hESC-hepa and hiPSC-hepa in detail.

In the present study, seven candidate genes (*FOXA2*, *HEX*, *HNF1α*, *HNF1β*, *HNF4α*, *HNF6*, and *SOX17*) were transduced into each stage of hepatic differentiation from hESCs by using an adenovirus (Ad) vector to screen for hepatic differentiation-promoting factors. Then, hepatocyte-related gene expression profiles and hepatocyte functions in hESC-hepa and hiPSC-hepa generated by the optimized protocol, were examined to investigate whether these cells have PHs characteristics. We used nine drugs, which are metabolized by various CYP enzymes and UDP-glucuronosyltransferases (UGTs), to determine whether the hESC-hepa and hiPSC-hepa have drug metabolism capacity. Furthermore, hESC-hepa and hiPSC-hepa were examined to determine whether these cells may be applied to evaluate drug-induced cytotoxicity.

Materials and methods

In vitro differentiation

Before the initiation of cellular differentiation, the medium of hESCs and hiPSCs was exchanged for a defined serum-free medium, hESF9, and cultured as previously reported [9]. The differentiation protocol for the induction of DE cells, hepatoblasts, and hepatocytes was based on our previous report with some modifications [5,6]. Briefly, in mesendoderm differentiation, hESCs and hiPSCs were dissociated into single cells by using Accutase (Millipore) and cultured for 2 days on Matrigel (BD biosciences) in differentiation hESF-DIF medium which contains 100 ng/ml Activin A (R&D Systems) and 10 ng/ml bFGF (hESF-DIF medium, Cell Science & Technology Institute; differentiation hESF-DIF medium was supplemented with 10 μg/ml human recombinant insulin, 5 μg/ml human apotransferrin, 10 μM 2-mercaptoethanol, 10 μM ethanolamine, 10 μM sodium selenite, and 0.5 mg/ml bovine serum albumin, all from Sigma). To generate DE cells, mesendoderm cells were transduced with 3000 VP/cell of Ad-FOXA2 for 1.5 h on day 2 and cultured until day 6 on Matrigel in differentiation hESF-DIF medium supplemented with 100 ng/ml Activin A and 10 ng/ml bFGF. For induction of hepatoblasts, the DE cells were transduced with each 1500 VP/cell of Ad-FOXA2 and Ad-HNF1α for 1.5 h on day 6 and cultured for 3 days on Matrigel in hepatocyte culture medium (HCM, Lonza) supplemented with 30 ng/ml bone morphogenetic protein 4 (BMP4, R&D Systems) and 20 ng/ml FGF4 (R&D Systems). In hepatic expansion, the hepatoblasts were transduced with each 1500 VP/cell of Ad-FOXA2 and Ad-HNF1α for 1.5 h on day 9 and cultured for 3 days on Matrigel in HCM supplemented with 10 ng/ml hepatocyte growth factor (HGF), 10 ng/ml FGF1, 10 ng/ml FGF4, and 10 ng/ml FGF10 (all from R&D Systems). In hepatic maturation, cells were cultured for 8 days on Matrigel in L15 medium (Invitrogen) supplemented with 8.3% tryptose phosphate broth (BD biosciences), 10% FBS (Vita), 10 μM hydrocortisone 21-hemisuccinate (Sigma), 1 μM insulin, 25 mM $NaHCO_3$ (Wako), 20 ng/ml HGF, 20 ng/ml Oncostatin M (OsM, R&D systems), and 10^{-6} M Dexamethasone (DEX, Sigma).

Results

Recently, we showed that the sequential transduction of SOX17, HEX, and HNF4α into hESC-derived mesendoderm, DE, and hepatoblasts, respectively, leads to efficient generation of the hESC-hepa [5–7]. In the present study, to further improve the differentiation efficiency towards hepatocytes, we screened for hepatic differentiation-promoting transcription factors. Seven candidate genes involved in liver development were selected. We then examined the function of the hESC-hepa and hiPSC-hepa generated by the optimized protocol for pharmaceutical use in detail.

Efficient hepatic differentiation by Ad-FOXA2 and Ad-HNF1α transduction

To perform efficient DE differentiation, T-positive hESC-derived mesendoderm cells (day 2) (Supplementary Fig. 1) were transduced with Ad vector expressing various transcription factors (Ad-FOXA2, Ad-HEX, Ad-HNF1α, Ad-HNF1β, Ad-HNF4α, Ad-HNF6, and Ad-SOX17 were used in this study). We ascertained the expression of *FOXA2*, *HEX*, *HNF1α*, *HNF1β*, *HNF4α*, *HNF6*, or *SOX17* in Ad-FOXA2-, Ad-HEX-, Ad-HNF1α-, Ad-HNF1β-, Ad-HNF4α-, Ad-HNF6-, or Ad-SOX17-transduced cells, respectively (Supplementary Fig. 2). We also verified that there was no cytotoxicity of the cells transduced with Ad vector until the total amount of Ad vector reached 12,000 VP/cell (Supplementary Fig. 3). Each transcription factor was expressed in hESC-derived mesendoderm cells on day 2 by using Ad vector, and the efficiency of DE differentiation was examined (Fig. 1A). The DE differentiation efficiency based on CXCR4-positive cells was the highest when Ad-SOX17 or Ad-FOXA2 were transduced (Fig. 1B). To investigate the difference between Ad-FOXA2-transduced cells and Ad-SOX17-transduced cells, gene expression levels of markers of undifferentiated cells, mesendoderm cells, DE cells, and extraembryonic endoderm cells were examined (Fig. 1C). The expression levels of extraembryonic endoderm markers of Ad-SOX17-transduced cells were higher than those of Ad-FOXA2-transduced cells. Therefore, we concluded that FOXA2 transduction is suitable for use in selective DE differentiation.

To promote hepatic commitment, various transcription factors were transduced into DE cells and the resulting phenotypes were examined on day 9 (Fig. 1D). Nearly 100% of the population of Ad-FOXA2-transduced cells and Ad-HNF1α-transduced cells was α-fetoprotein (AFP)-positive (Fig. 1E). We expected that hepatic commitment would be further accelerated by combining FOXA2 and HNF1α transduction. The DE cells were transduced with both Ad-FOXA2 and Ad-HNF1α, and then the gene expression levels of *CYP3A7* [10], which is a marker of fetal hepatocytes, were evaluated (Fig. 1F). When both Ad-FOXA2 and Ad-HNF1α were transduced into DE cells, the promotion of hepatic commitment was greater than in Ad-FOXA2-transduced cells or Ad-HNF1α-transduced cells.

To promote hepatic expansion and maturation, we transduced various transcription factors into hepatoblasts on day 9 and 12 and the resulting phenotypes were examined on day 20 (Fig. 1G). We ascertained that the hepatoblast population was efficiently expanded by addition of HGF, FGF1, FGF4, and FGF10 (Supplementary Fig. 4). The hepatic differentiation efficiency based on asialoglycoprotein receptor 1 (ASGR1)-positive cells was measured on day 20, demonstrating that FOXA2, HNF1α, and HNF4α transduction could promote efficient hepatic maturation (Fig. 1H). To investigate the phenotypic difference between Ad-FOXA2-, Ad-HNF1α-, and Ad-HNF4α-transduced cells, gene expression levels of early hepatic markers, mature hepatic markers, and biliary markers were examined (Fig. 1I). Gene expression levels of mature hepatic markers were up-regulated by FOXA2, HNF1α, or HNF4α transduction. FOXA2 transduction strongly upregulated gene expression levels of both early hepatic markers and mature hepatic markers, while HNF1α or HNF4α transduc-

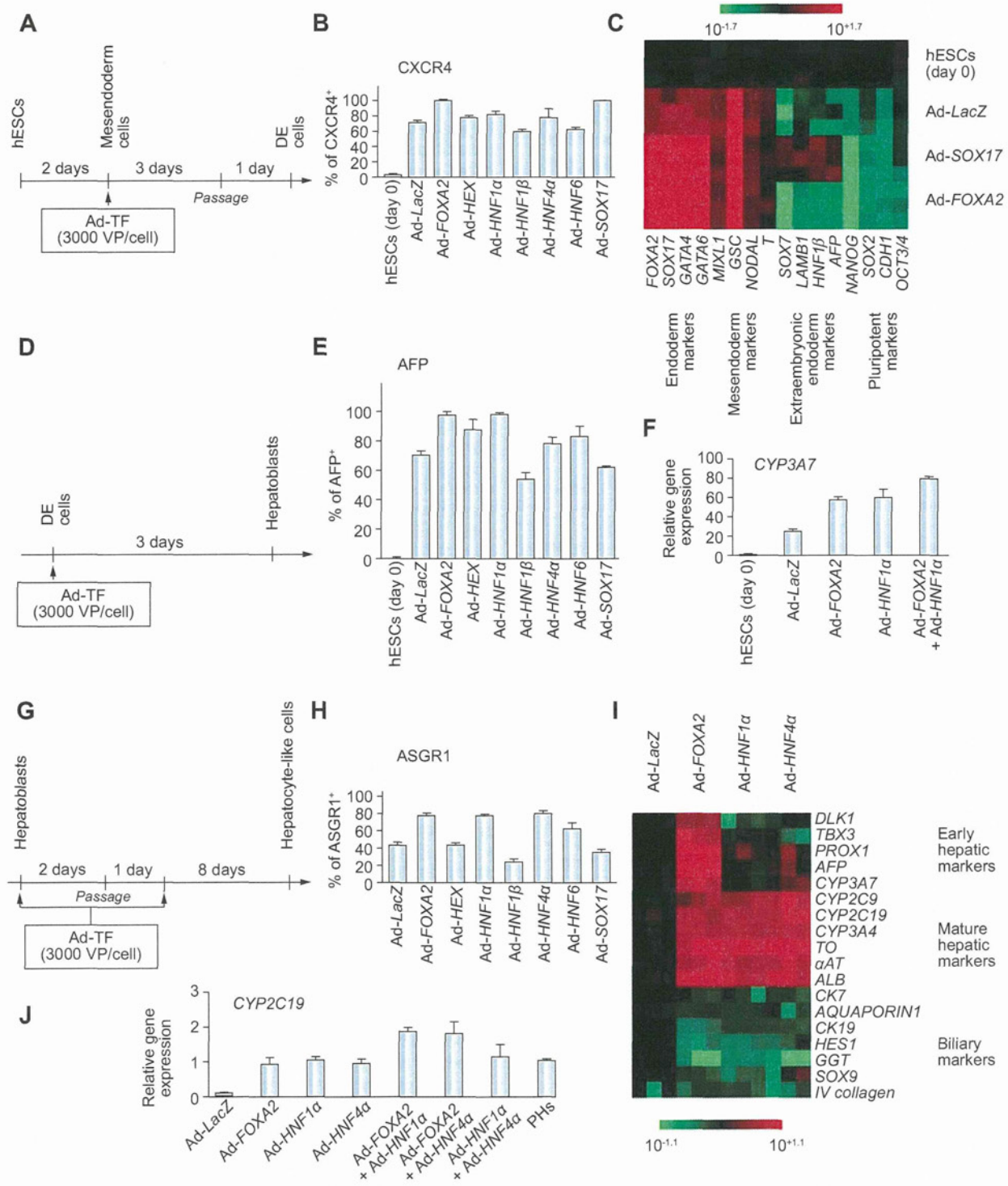

Fig. 1. Efficient hepatic differentiation from hESCs by FOXA2 and HNF1α transduction. (A) The schematic protocol describes the strategy for DE differentiation from hESCs (H9). Mesendoderm cells (day 2) were transduced with 3000 VP/cell of transcription factor (TF)-expressing Ad vector (Ad-TF) for 1.5 h and cultured as described in Fig. 2A. (B) On day 5, the efficiency of DE differentiation was measured by estimating the percentage of CXCR4-positive cells using FACS analysis. (C) The gene expression profiles were examined on day 5. (D) Schematic protocol describing the strategy for hepatoblast differentiation from DE. DE cells (day 6) were transduced with 3000 VP/cell of Ad-TF for 1.5 h and cultured as described in Fig. 2A. (E) On day 9, the efficiency of hepatoblast differentiation was measured by estimating the percentage of AFP-positive

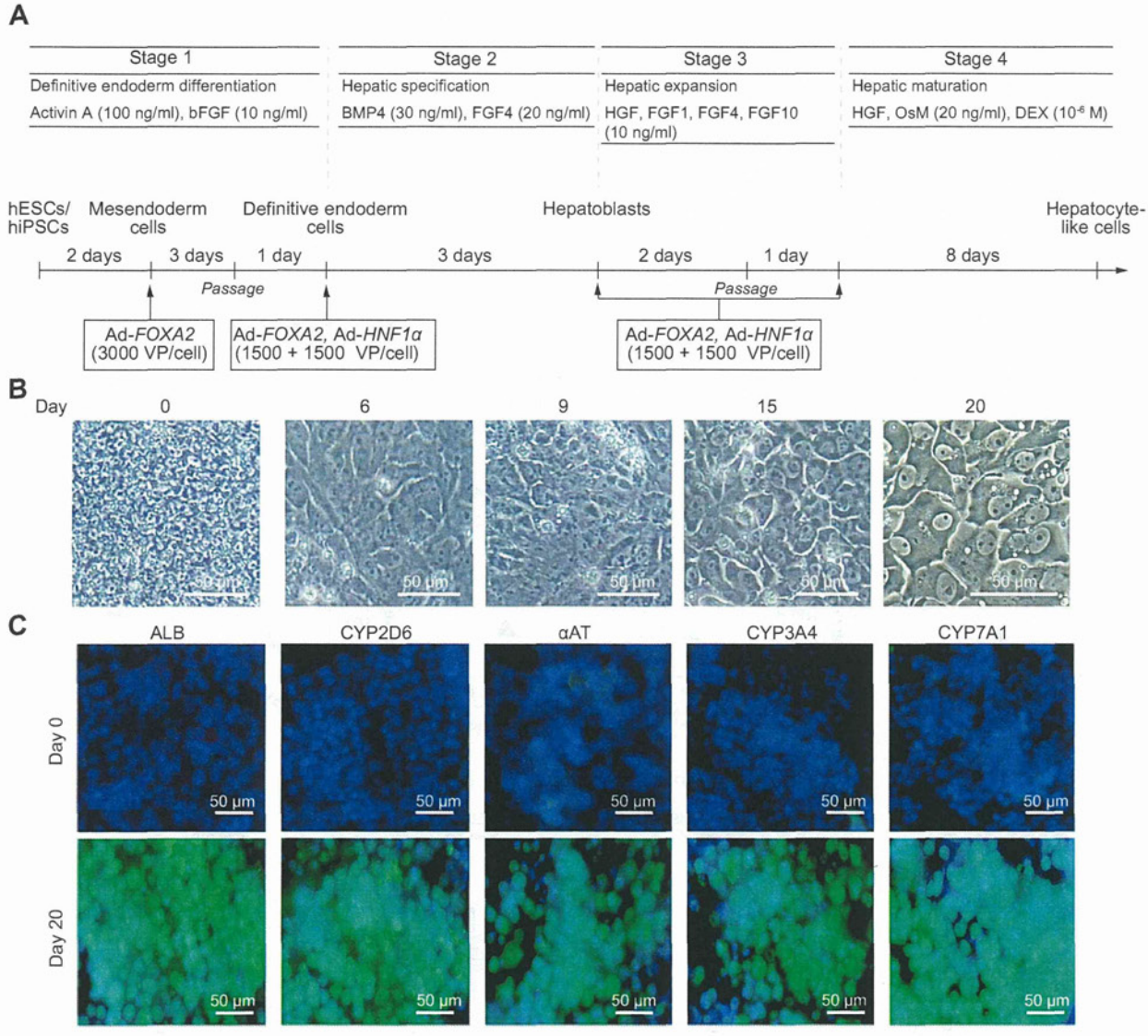

Fig. 2. Hepatic differentiation of hESCs and hiPSCs by FOXA2 and HNF1α transduction. (A) The differentiation procedure of hESCs and hiPSCs into hepatocytes via DE cells and hepatoblasts is schematically shown. Details of the hepatic differentiation procedure are described in Materials and methods. (B) Sequential morphological changes (day 0–20) of hESCs (H9) differentiated into hepatocytes are shown. (C) The expression of the hepatocyte markers (ALB, CYP2D6, αAT, CYP3A4, and CYP7A1, all green) was examined by immunohistochemistry on day 0 and 20. Nuclei were counterstained with DAPI (blue).

tion did not up-regulate the gene expression levels of early hepatic markers. Next, multiple transduction of transcription factors was performed to promote further hepatic maturation. The combination of Ad-FOXA2 and Ad-HNF1α transduction and the combination of Ad-FOXA2 and Ad-HNF4α transduction result in the most efficient hepatic maturation, judged from the gene expression levels of *CYP2C19* (Fig. 1J). This may happen because the mixture of immature hepatocytes and mature hepatocytes coor-

cells using FACS analysis. (F) The gene expression level of *CYP3A7* was measured by real-time RT-PCR on day 9. On the *y* axis, the gene expression level of *CYP3A7* in hESCs (day 0) was taken as 1.0. (G) The schematic protocol describes the strategy for hepatic differentiation from hepatoblasts. Hepatoblasts (day 9) were transduced with 3000 VP/cell of Ad-TF for 1.5 h and cultured as described in Fig. 2A. (H) On day 20, the efficiency of hepatic differentiation was measured by estimating the percentage of ASGR1-positive cells using FACS analysis. The detail results of FACS analysis are shown in Supplementary Table 1. (I) Gene expression profiles were examined on day 20. (J) Hepatoblasts (day 9) were transduced with 3000 VP/cell of Ad-TFs (in the case of combination transduction of two types of Ad vector, 1500 VP/cell of each Ad-TF was transduced) for 1.5 h and cultured. Gene expression levels of *CYP2C19* were measured by real-time RT-PCR on day 20. On the *y* axis, the gene expression level of *CYP2C19* in PHs, which were cultured for 48 h after the cells were plated, was taken as 1.0. All data are represented as mean ± SD (n = 3).

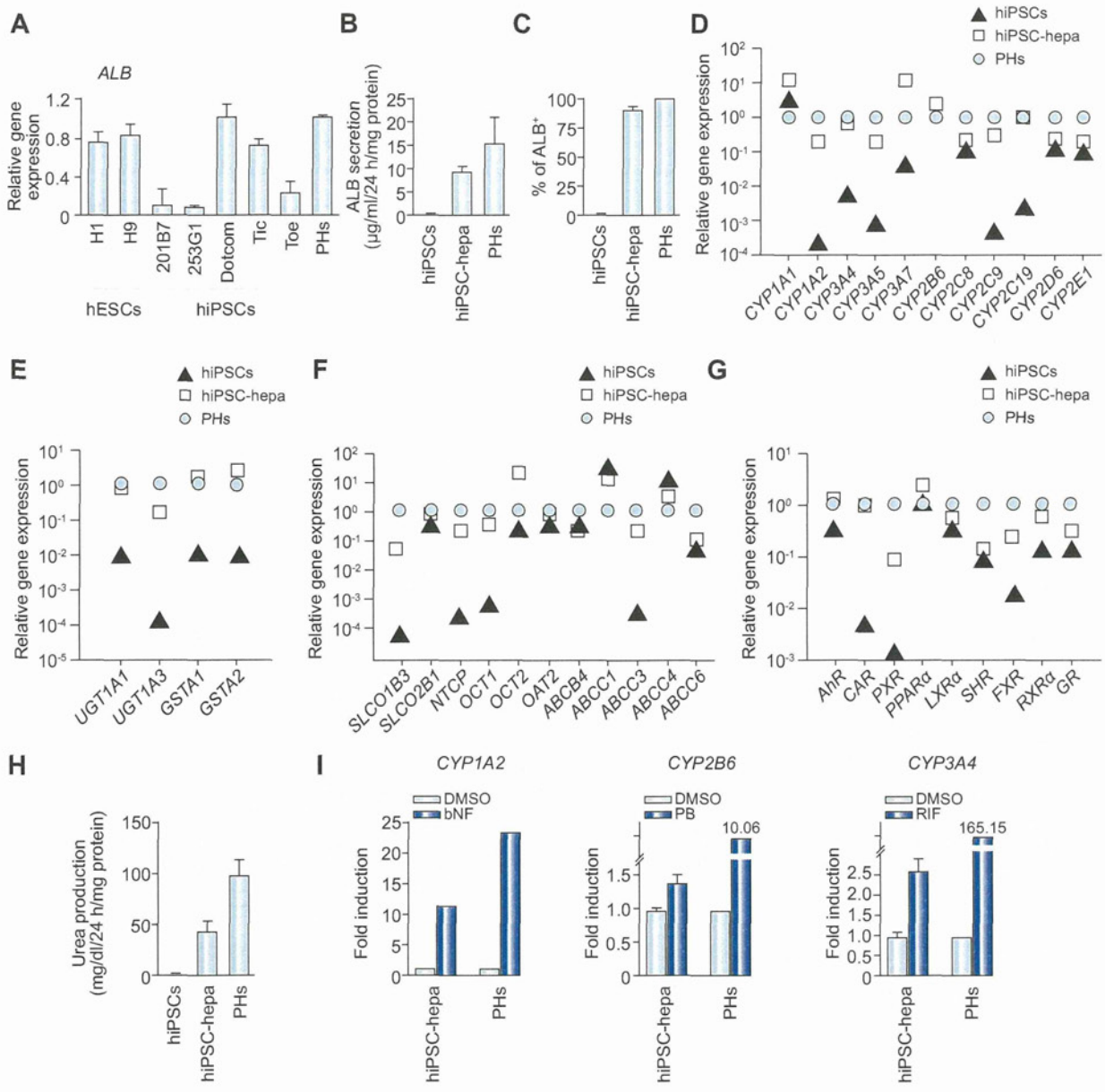

Fig. 3. The hepatic characterization of hiPSC-hepa. hESCs (H1 and H9) and hiPSCs (201B7, 253G1, Dotcom, Tic, and Toe) were differentiated into hepatocyte-like cells as described in Fig. 2A. (A) On day 20, the gene expression level of *ALB* was examined by real-time RT-PCR. On the *y* axis, the gene expression level of *ALB* in PHs, which were cultured for 48 h after cells were plated, was taken as 1.0. (B–I) hiPSCs (Dotcom) were differentiated into hepatocyte-like cells as described in Fig. 2A. (B) The amount of ALB secretion was examined by ELISA in hiPSCs, hiPSC-hepa, and PHs. (C) hiPSCs, hiPSC-hepa, and PHs were subjected to immunostaining with anti-ALB antibodies, and then the percentage of ALB-positive cells was examined by flow cytometry. (D–G) The gene expression levels of CYP enzymes (D), conjugating enzymes (E), hepatic transporters (F), and hepatic nuclear receptors (G) were examined by real-time RT-PCR in hiPSCs, hiPSC-hepa, and PHs. On the *y* axis, the expression level of PHs is indicated. (H) The amount of urea secretion was examined in hiPSCs, hiPSC-hepa, and PHs. (I) Induction of *CYP1A2*, *2B6*, or *3A4* by DMSO or inducer (bNF, PB, or RIF) of hiPSC-hepa and PHs, cultured for 48 h after the cells were plated, was examined. On the y axis, the gene expression levels of *CYP1A2*, *2B6*, or *3A4* in DMSO-treated cells, which were cultured for 48 h, were taken as 1.0. All data are represented as mean ± SD (n = 3).

dinately works to induce hepatocyte functions. Taken together, efficient hepatic differentiation could be promoted by using the combination of FOXA2 and HNF1α transduction at the optimal stage of differentiation (Fig. 2A). At the stage of hepatic expansion and maturation, Ad-HNF4α can be substituted for Ad-HNF1α (Fig. 1J). Interestingly, cell growth was delayed by FOXA2 and HNF4α transduction (Supplementary Fig. 5). This delay in cell proliferation might be due to promoted maturation by FOXA2 and HNF1α transduction. As the hepatic differentiation proceeds, the morphology of hESCs gradually changed into a typical hepatocyte morphology, with distinct round nuclei and a polygonal shape (Fig. 2B), and the expression levels of hepatic markers